2010-01-01

Coincident Visual Retinotopy In Simultaneous Slow Cortical Potentials And Fmri Recordings

Hugo Sandoval
University of Texas at El Paso, guayosandoval@gmail.com

COINCIDENT VISUAL RETINOTOPY IN SIMULTANEOUS SLOW CORTICAL POTENTIALS AND fMRI RECORDINGS:

VALIDATION OF EEG AS AN IMAGING TOOL

HUGO SANDOVAL

Department of Biological Sciences

APPROVED

_____
Louis N. Irwin, Ph.D.

_____
Kristin L. Gosselink, Ph.D.

_____
Max Shpak, Ph.D.

_____
Stephen F. Sands, Ph.D.

_____
Patricia D. Witherspoon, Ph.D.
Dean of the Graduate School

Dedication

To my family and friends

COINCIDENT VISUAL RETINOTOPY IN SIMULTANEOUS SLOW CORTICAL POTENTIALS AND fMRI RECORDINGS:

VALIDATION OF EEG AS AN IMAGING TOOL

By

HUGO SANDOVAL

DISSERTATION

Presented to the Faculty of the Graduate School of

The University of Texas at El Paso

in Partial Fulfillment

of the Requirements

for the Degree of

DOCTOR OF PHILOSOPHY

Department of Biological Sciences

THE UNIVERSITY OF TEXAS AT EL PASO

December 2010

Acknowledgments

I would like to thank Dr. Donald Moss, Dr. Stephen Sands, and Dr. Louis Irwin, for sharing their knowledge and passion, for their time, patience, and support. I would also like to thank Dr. Kristin Gosselink, Dr. Max Shpak, and Andrew Sands for their unconditional help.

Abstract

Slow Cortical Potentials (SCPs) and Evoked Potentials (EP) in combination with source reconstruction techniques can provide accurate and essential information about brain activity. Current techniques offer the necessary tools to study the human brain by providing detailed temporal and spatial information of the normal brain and its disorders. Human functional neuroimaging currently uses fMRI as the gold standard because of its high spatial localization and because of being non-invasive. This method's disadvantages are its high cost and unnatural environment. The purpose of this work was to determine if the combination of SCPs and traditional electroencephalography (EEG) provides a suitable technique to study the temporal and spatial localization of brain activity. I propose the application of EEG, SCPs, and source reconstruction as an alternative to fMRI brain mapping. This study provides supporting evidence for the application of EEG and SCPs not only as an alternative but also as a complementary technique which can provide the temporal details missing from fMRI data. During this work, localization equivalent to that obtained from fMRI was achieved by combining EEG and source localization. I provide ample evidence that a high level of spatial detail can be achieved by combining high density EEG recordings, and slow cortical potentials with accurate source reconstruction techniques.

Table of Contents

List of Figures

List of Tables

Chapter 1

INTRODUCTION

In this precise moment, as you scan these words, visual information is traveling at high speeds to your visual cortex where your brain is making sense of what is being described. The left inferior-frontal gyri also referred to as Broca's Area and the left parieto-temporal area or Wernicke's area analyze the words while the occipito-temporal area recognizes the words. The detailed information we have about where, how, and when these events take place in our brain is a result of the combination of different brain mapping methodologies which have been discovered and perfected during the last three decades.

Even though we currently have a wide range of brain mapping techniques available, each of them has limitations, and only their sum and integration can provide a very accurate and detailed representation of brain anatomy and function.

Toga and Mazziotta (2007) describe the ideal brain mapping technique in their Brain Mapping Methods Textbook as follows:

> "The ideal brain mapping technique would have extremely high spatial and temporal resolution with a capacity to sample a large volume of the brain continuously. Its cost would be low as would its invasiveness, making it applicable in many settings, in human subjects as well as in animal models". Presently, this technique is not available.

The purpose of my study was to determine if the combination of Slow Cortical Potentials (SCPs) and traditional electroencephalography (EEG) can provide this ideal technique. To do so, a series of studies was conducted to determine if EEG can provide high spatial and temporal resolution and sample a large volume of the brain continuously, at a low cost, with minimum invasiveness, in different settings, in human subjects.

In regard to spatial resolution, the power of EEG is usually underappreciated. In the results and discussion section, I provide ample evidence that a high level of spatial detail can be achieved by combining high density EEG recordings with accurate source reconstruction techniques. With respect to time, EEG is the method of choice because of its msec resolution.

To address the issue of sampling large brain volumes continuously, this study includes the SCP portion of the EEG signal and extends the traditional analysis timeframe from msecs to 30 secs. Similar studies in our laboratory have used a similar methodology with analysis times of several minutes very successfully. With respect to cost, the equipment price for EEG is approximately 5% of the cost of functional Magnetic Resonance Imaging (fMRI) or Positron Emission Tomography (PET). Differences in cost per person per study as well as equipment maintenance and running costs are also approximately 95% less for EEG. These factors make EEG ideal for imaging studies.

EEG recordings can be conducted in almost any setting and situation, because they are done using a portable and non-invasive device. This is a limitation for fMRI, Magneto encephalography (MEG), and PET which are conducted in an unnatural environment and with the use of radiation in the case of PET. Another advantage of EEG is the long history and variety of electrophysiology studies performed in different animal models. I propose that SCPs within the EEG signal can be applied to study the human brain with the highest temporal resolution, in the msec range, with acceptable spatial resolution in the centimeter to millimeter range. SCPs provide meaningful information that is usually ignored with traditionally filtered EEG studies, since low frequency components in the range of 1 to 70 Hz are measured by EEG studies making use of fuller bandwidths. This technique can be applied broadly for cognitive neuroscience and for clinical testing in a natural human environment. On the cognitive

application side, SCPs can provide a better understanding of how different brain areas are associated with different functions like learning, memory, attention, and basic sensory neurophysiology. Some of the major clinical applications of SCPs include evaluation of brain function in newborns, brain damage after trauma, and response to therapy or to treatment in Attention Deficit disorders. It can also be used to scale brain atrophy in neurodegenerative diseases such as Alzheimer's and Parkinson's Diseases. These clinical and cognitive applications make the development and understanding of SCP fundamental.

Presently, the most common method used to image the human brain is functional Magnetic Resonance Imaging (fMRI). It offers the best spatial resolution available, but at a multimillion dollar cost per instrument in an uncomfortable and unrealistic environment. This and other major imaging techniques are described below, providing a context for the utility of EEG and SCPs. My results support the application of EEG and SCP as an accurate, affordable, and portable alternative method for mapping the human brain which is not far from the ideal technique previously described.

A. IMAGING METHODS

1. Anatomical Magnetic Resonance Imaging (MRI)

MRI's initial developments took place in the 1970's, and its expansion to anatomical MRI happened in the 1980's. The production of high resolution structural images of organs is based on the nuclear momentum properties of an atom, usually of hydrogen, since the human brain as well as the body has an abundance of water (De Yoe et al., 1994). By manipulating these nuclear momentum properties with the use of radio-frequency irradiation, and applying a series of physical and mathematical transformations, brain and body images with pristine spatial

resolution are obtained. These brain images with exquisite anatomical detail are used to overlay functional results and obtain a high spatial resolution representation of neural activity. The main advantage of anatomical MRI is the capacity to obtain millimeter detail in a non invasive and risk-free way (De Yoe et al., 1994).

2. Functional Magnetic Resonance Imaging (fMRI)

fMRI also relies on the protons of water as the signal source. The exact relationship between fMRI and brain activity is not clear at the moment, but hemodynamic changes occur unequivocally every time neural activity increases. The fMRI signal is a direct measurement of blood oxygenation and a reliable and consistent indirect measurement of neural activity (He & Raichle, 2009). When neural activity increases, the blood oxygen level-dependent (BOLD) signal increases (Logothetis et al., 2001). The major limitations of fMRI are that it is an indirect measurement of neural activity and its temporal resolution is limited by the hemodynamic response. Some of its advantages are its capacity to localize superficial and deep neural activity with millimeter spatial resolution in a noninvasive and risk-free way (Ogawa et al., 1998).

3. Positron Emission Tomography (PET)

PET is a specialized molecular imaging technique. It uses radioactive probes which tag the molecule of interest, which then is introduced into the body by intravenous injection. Radiation emitted by a particular body part will be detected and measured by external detectors. Fluorine-18 is used as the isotope to perform studies of glucose consumption. This measurement is very useful for the early detection of tumors. It is also used to study neural activity by measuring glucose metabolism. H-15 is the isotope of choice to study brain hemodynamic response. PET's major advantage is its capacity to detect cancer in very early stages. It is also very useful for

localizing superficial and deep neural activity with good spatial resolution although not as good as fMRI. Unfortunately, PET is invasive and involves the use of ionizing radiation (Sossi, 2003).

4. Magnetoencephalography (MEG)

MEG uses sensitive detectors to record the weak magnetic fields generated by brain currents. One advantage of MEG over EEG is that MEG can detect cortical activity directly through the skull, without the distortion imposed by the scalp and the skull on EEG potentials. The source of the MEG signal is similar to that of EEG, which is the postsynaptic current from cortical pyramidal cells and the main advantages of this technique include its high temporal resolution in the msec range, being non invasive, risk free, and a direct measurement of neural activity. The major limitations are the non natural environment imposed by the sensor array and the magnetically shielded room required for collecting the data, and the fact that if deep signals are attenuated, source reconstruction modeling is necessary. In addition, since MEG detectors are not fixed to the head, it is necessary to use head position measurements (Malmivuo, 2005).

B. ELECTROENCEPHALOGRAPHY

1. History

The origins of EEG date back to 1874, when Richard Caton used a galvanometer to measure the electrical signals from a rabbit's brain (Brazier, 1957). In the early 1920's, Hans Berger was the first to record EEG from humans. The first EEG recordings were just coarse small shadows of brain waves recorded with a small galvanometer (Millett, 2001). Since then, conventional EEG has been applied to study human brain neurophysiology and pathophysiology.

EEG represents spatially summed and volume conducted local field potentials (Menon and Crottaz-Herbette, 2005). A common application of EEG is to average its response to a repeated stimulus. This application is known as Event Related Potentials (ERP), and was introduced by Herbert G. Vaughan in 1969. With this methodology, a specific brain response to a particular event can be determined. ERPs were classified by Vaughan into the following categories: sensory, motor and, long latency potentials, and steady potential shifts (Andreassi, 1995). During this study, I conducted sensory ERP studies of the visual system.

2. Slow Cortical Potentials

SCPs are brain waves oscillating at frequencies below 0.5 Hertz in the EEG signal. The source of SCP has been mainly attributed to postsynaptic potentials of pyramidal neurons (Birbaumer, 1999). These slow wave shifts in the EEG signal can only be detected when recorded with DC amplifiers, and most of the time even when DC amps are used during routine EEG studies, SCPs are filtered out. Since physiological and pathological EEG activity occurs in ranges from 0.01 to several hundred hertz, important information is overlooked when SCPs are filtered out (Vanhatalo, et al., 2005).

Slow waves are generated mainly in neocortical pyramidal cells, which approximate 85% of cortical neurons (Braitenberg & Schuz, 1991), located directly underneath or in close proximity to the recording electrode (Khader, 2008). SCPs precede and follow stimulus presentation (Roesler et al., 1997). For SCP studies the time range of interest is 500 msecs before to several seconds after the stimulus (Kahder et al., 2005). In comparison, ERP studies detect short living components with well defined peaks in a time range of 10 to 500 msecs.

Human EEG recordings in the past were not capable of recording SCPs because electrode and amplifier drifts saturated the amplifier's dynamic range (Vanhatalo et al., 2005). Presently, however, current technology can record full bandwidth EEG signals and help us understand how the brain works. To record slow cortical potentials, the amplifiers need to meet the following criteria: they must be DC coupled, DC stable, and have a wide dynamic range (Vanhatalo et al, 2005). Since amplifiers with these characteristics have been readily available only recently, the study of SCPs with a higher number of channels is just emerging as an imaging technique, even though SCP studies have been recorded since the early sixties. Following are some of the first studies:

Breitschaftspotential (BP). BPs are movement related potentials which precede volitional movement in humans. They were discovered by Kornhuber and Deecke in 1964. They are also called readiness potentials, consisting of an early component BP1 and a late component BP2. BP1 is mainly generated by the supplementary and cingulate motor areas, while BP2 is mainly generated by primary motor cortex. BP1 appears approximately 1.5 sec before the onset of the electromyogram (EMG) reflecting muscle contraction, while BP2 is generated about 0.5 sec before EMG onset (Cui, 2000). The amplitude of the BP is maximal over the motor cortex representation of the moving limb. For finger and hand movements, maximum contralateral activations were observed, and for foot movement maximum ipsilateral activations were observed. The amplitude of the negativity increases with movement complexity (Birbaumer. 1990). Shibasaki and Hallett (2006) report that both components of the readiness potential are related to preparation and execution of voluntary movements (Shibasaki and Hallett, 2006).

Contingent Negative Variation (CNV). During CNV, DC potentials precede a stimulus which requires a fast button press. A warning signal is provided before the stimulus is presented. During the time between warning and stimulus, slowly changing negative potentials are observed (Birbaumer, 1990). In the pioneering experiment of Walter et al (Walter et al., 1964); a flash was used as a conditional stimulus and a series of clicks followed as an imperative stimulus. The CNV was mostly present in anterior brain locations (Walter et al., 1964). A broader scope of SCP applications is discussed in the following section.

3. Slow Cortical Potential Applications

As an alternative to other brain imaging techniques in a more natural environment. Evidence from the literature supports the relationship and similar topographical specificity between SCPs and blood oxygen level-dependent fMRI responses during different cognitive imaging studies (Khader, 2008). This is evidence of how SCPs can be used as an alternative to fMRI to achieve a better understanding of human neuroanatomy and neurophysiology, with the advantage of being portable and not requiring the subject to lay in a closed chamber as for fMRI and PET.

Plasticity. SCPs have been used to study brain plasticity and cortical reorganization. Different overall topography of SCPs was observed in a study of slow event related brain potentials in blind and sighted adult human subjects during a haptic mental rotation paradigm. Occipital areas were activated in the blind population during tactile stimulus encoding, while pronounced frontal activation was observed in the sighted population (Roesler et al., 1993). SCPs were also used to study plasticity in the cortex during piano practice. SCP results showed

that the anterior right hemisphere provides audio-motor interface for the mental representation of the keyboard (Bangert and Altenmuller, 2003). The results of this study exemplify the application of SCPs as a technique to study the biological substrates of brain reorganization associated with plasticity, which are still not completely understood.

Neonatal brain evaluation. Vanhatalo et al., (2002) proposed the application of SCPs to asses physiological and pathophysiological neonatal brain function since it can be performed easily at the bedside of human infants (Vanhatalo et al., 2002). The presence of pronounced and slow activity patterns in human neonates and immature brain tissue in different species might reflect functional and structural shaping of neuronal circuits. In a study of preterm EEG brain activity it was found that the dominating frequency range was 0.01 to 0.1 Hertz (Vanhatalo et al., 2005). SCP spectral analysis has also been applied as a diagnostic tool for sick neonates where a hypoactive left lower frontal activity is observed (Thordstein, 2004). These studies are examples of how a better understanding of SCPs can be used more reliably and widely to assess physiology and pathophysiology of the neonate brain (Vanhatalo et al., 2002).

Memory. SCPs have also been applied to the study of human memory. In research by Khader et al., (2005b), SCPs were associated with long-term memory representation of faces and spatial position with different topographies. More negative potentials were observed over parietal and occipital areas during recall of positions, while central and frontal electrodes detected more negative potentials during recall of faces (Khader, 2005b). The same group conducted an fMRI study with a similar experimental design. Their fMRI results showed parietal and pre-central cortex activations during position recall and posterior cingulate cortex for face recognition. Slow negative EEG shifts were observed during memory retrieval. The onset of the shifts corresponded with the stimulus presentation and went back to baseline a few

seconds after the overt response. Amplitude was directly proportional to the degree of difficulty of the stimuli (Khader et al., 2005a). In a previous study by the same group, SCPs were recorded to study long term memory retrieval where subjects were trained to associate pictures with spatial position, pictures with color conditions, and pictures with verbal conditions. The negative maximum SCP was found over parietal cortex for spatial conditions, over occipital to temporal cortex for color, and over left frontal cortex for verbal information. These results support the pre-established concept of memory representation reactivating cortical processing areas (Roesler, 1995). During autobiographical memory retrieval, areas over the left frontal lobe showed marked negative DC shifts during retrieval, while a similar but smaller effect was observed over the right frontal lobe. Subjects were also instructed to hold the memories in mind, resulting in negative shifts in the posterior temporal and occipital cortex (Conway, 2001). SCPs have also been used to study short term memory. Results indicated that the manipulation of verbal information occurs in the left frontal cortex, while spatial information manipulation occurs in the parietal cortex (Rolke et al., 2000).

Treatment of Epilepsy. SCP regulation can be used as an alternative treatment for drug-refractory epilepsy; where patients learn to discriminate between negative or positive polarizations and later are taught to regulate their SCPs to reduce or completely eliminate the number of seizures (Birbaumer 1999, Strehl, 2006).

Attention Deficit/Hyperactivity Disorder (ADHD). Self regulation of SCPs can also be used to treat ADHD. During the self regulation training, SCP increases and decreases are fed back visually and auditorily while children learn to regulate their SCPs (Strehl, 2006). The major conclusion from the study of attention using SCPs by Basile et al. (2006) was to recommend

caution when doing group studies using SCPs, since a high degree of subject variability was observed.

All of the previous examples illustrate the variety of applications and the importance and value of SCP as a brain imaging tool.

4. EEG and the BOLD Signal

Is there a close correspondence between SCPs and the BOLD signal? Is this correspondence based on neural activity? Evidence from the literature supports a tight correspondence between SCPs and the BOLD signal and its neural source. A study of single digit multiplication showed how the topography of slow negative waves varied with the complexity of the multiplication; SCPs were more pronounced with larger multiplications (Jost, 2004). The amplitude of slow waves (Roesler et al., 1997) and of the BOLD response (Khader et al., 2008) was both directly proportional to the effort involved with the task. A strong correspondence between the BOLD response and SCPs is also presented by Khader et al., (2008) during human imagery studies. Very specific similarities between SCPs of less than 1 Hz. and BOLD responses have been described by Kahder et al. (2008). Both modalities showed increased signal strength with increased difficulty. These similarities as well as the association of post-synaptic-potentials with both signals are evidence of a direct correspondence between the BOLD signal and the SCP.

The EEG signal is directly related to neural processing, while the BOLD response is an indirect measure of neural activity, reflecting blood flow changes associated with brain activity (Logothetis et al., 2001). Since the fMRI signal is highly correlated with local field potentials (Logothetis et al., 2001) and the EEG reflects spatially summed local field potentials (Menon and Crottaz-Herbette, 2005), these two complementary techniques provide information about similar

as well as different biological substrates, so their combination can provide a better representation of the same neural response.

5. The Inverse Problem and sLORETA.

The main limitation to every EEG study is the inverse problem, where there are an infinite number of possible "solutions" for a particular scalp electrical potential. By this is meant that, in principle, many combinations of neuronal activity originating from many locations in the brain could give rise to the observed EEG pattern. A unique solution to the intracranial current source of the scalp recorded EEG signal can only be estimated. However, current source reconstruction models can provide excellent localization by limiting solutions to the brain cortex, with just a single or a few dipole sources (Scherg, 1990). During these studies, simultaneous EEG and fMRI signals were used to independently verify the dipole sources.

Standardized low resolution brain electromagnetic tomography (sLORETA) is a method that provides a satisfactory solution to the inverse problem by computing an estimate of the location, orientation, and strength of the electrical generators with no error. sLORETA is used to compute EEG statistical maps which indicate the source location for a particular process with zero localization error. It provides first order localization and is used to calculate a 3D cortical distribution of current density. It uses a mathematical model that maximizes the synchronization of strength between neighboring neuronal populations. Localization inference is based on a standardization of current density estimates. When compared with other source reconstruction techniques, like Dale and the minimum norm, sLORETA (Pascual-Marqui, 2002) was the only one which achieved zero localization error on the noise free simulations. Because of this advantage, sLORETA was used for source reconstruction. sLORETA has been validated by

showing consistent 3D localization results with well established neurophysiological studies of vision, audition, and language (Pascual-Marqui, 2002).

6. Retinotopic Maps

The response to visual stimulus follows an orderly fashion. This order follows the representation and processing of different areas of the visual field to particular locations in the primary visual cortex. Stimuli to the left upper visual field are inverted at the lens and are processed in the inferior right area of primary visual cortex. In the same fashion, stimuli to the left lower visual field are represented in the superior right visual cortex, while the right upper visual field is represented in the left lower area of primary visual cortex, and the right lower visual field is represented in the left upper area of primary visual cortex (Posner & Raichle, 1994). This precise and well known retinotopic organization of the visual cortex was selected for these studies to determine if EEG can be used to generate retinotopic maps.

Chapter 2

EXPERIMENTAL DESIGN

A. AIMS

1. General Aims.

The main purpose of this study was to evaluate the application, benefits and weaknesses of EEG as an imaging tool. To do so, the following questions were addressed: (1) Can SCPs combined with ERP studies and accurate source localization, provide adequate spatial resolution and be established as an alternative to PET and fMRI? (2) Would these results be comparable to simultaneous EEG/fMRI studies? (3) Is there a close correspondence between SCPs and the BOLD signals?

The strategy used to answer these questions consisted of presenting a visual stimulus to each of the four visual quadrants to human subjects, to construct retinotopic maps for each quadrant of the visual field. Each study employed three different measurements: a 10 sec Slow Cortical Visual Evoked Potential (VEP), a 30 sec Slow Cortical VEP, and Simultaneous EEG/fMRI retinotopic mapping for 30 secs.

2. Specific Aims

Specific Aim I - To asses the effectiveness of EEG as an imaging tool. To determine if EEG with adequate source reconstruction techniques can provide accurate spatial and temporal information on brain function, a simultaneous EEG/fMRI visual study was conducted. A well established organization of the visual cortex into visual field maps has been identified with the application of modern neuroscience techniques like fMRI and PET. In order to validate EEG as

an imaging tool, EEG and fMRI measurements of human visual field maps were recorded and compared with the existing retinotopic maps.

Specific Aim II - To determine if conventional EEG methods overlook brain activation with a slower time course. To accomplish this objective, VEPs and SCPs below 1 Hz were studied with retinotopic map representation of human visual fields.

Specific Aim III - To determine if the duration of the stimulus trains has an effect on the SCP and VEP. This was analyzed through measurements over a short 10 second duration interval and a longer 30 second duration interval.

B. EXPERIMENT 1

1. Subjects

Four normal adult male volunteers at 37, 40, 44, and 55 years of age were recruited from the local community and from the University of Texas at El Paso. All subjects gave informed consent before participating in accordance with the guidelines of the local Institutional Review Board (Appendix A).

2. EEG Subject Preparation

An explanation of the experiment was given to the subjects. Every subject read and signed the Human Subject Consent form (Appendix A) and completed the Human Subject Personal Information Form. Subjects brushed their scalp to remove any dead skin cells. Next, an Electrode Array EEG cap was placed over the subjects head. The Cz electrode was aligned with the left and right preauricular points. Once the cap was aligned, conductive gel was added to each electrode and the skin under each electrode was abraded until impedances of 5 K Ohms or

lower were achieved. After this procedure was completed, EEG recording and stimulus presentation began.

3. EEG Recordings

EEG was recorded with a DC amplifier. Sintered silver/ silver chloride electrodes were used because of their ideal DC stability, superior low frequency noise, and low resistance (Tallgren, 2005). Sixty-eight electrode locations were used using the left ear as a common reference. The amplifier's bandpass range was DC to 200 Hz and the digitization rate was 1000 Hz. Scalp electrode positions were based on the 10-10 extension to the 10-20 positioning system by Jasper (Oostenveld and Praamstra, 2001). EEG recordings were conducted while the subjects lay in the scanner bed.

4. EEG/fMRI Visual Stimulus Presentation

The stimulus was generated by using a Dell computer using software developed at Sands Research and was projected with a Magnetic Resonance compatible visual projection. Visual stimuli consisted of a total of 10 repetitions of 30 sec block stimuli with 90 checkerboard presentations per train per quadrant. The stimulus consisted of a 60 degree black and white flickering checkerboard radial wedge presented to each quadrant (Figure 1). The stimulus had a gray background and a yellow crosshair in the center and the stimulus duration for each checkerboard was 50 msecs. Subjects were instructed to stare at a yellow crosshair while watching the checkerboard pattern reversal. To preserve this pre-stimulus baseline during these studies an inter-stimulus interval of 10 ± 5 sec was used.

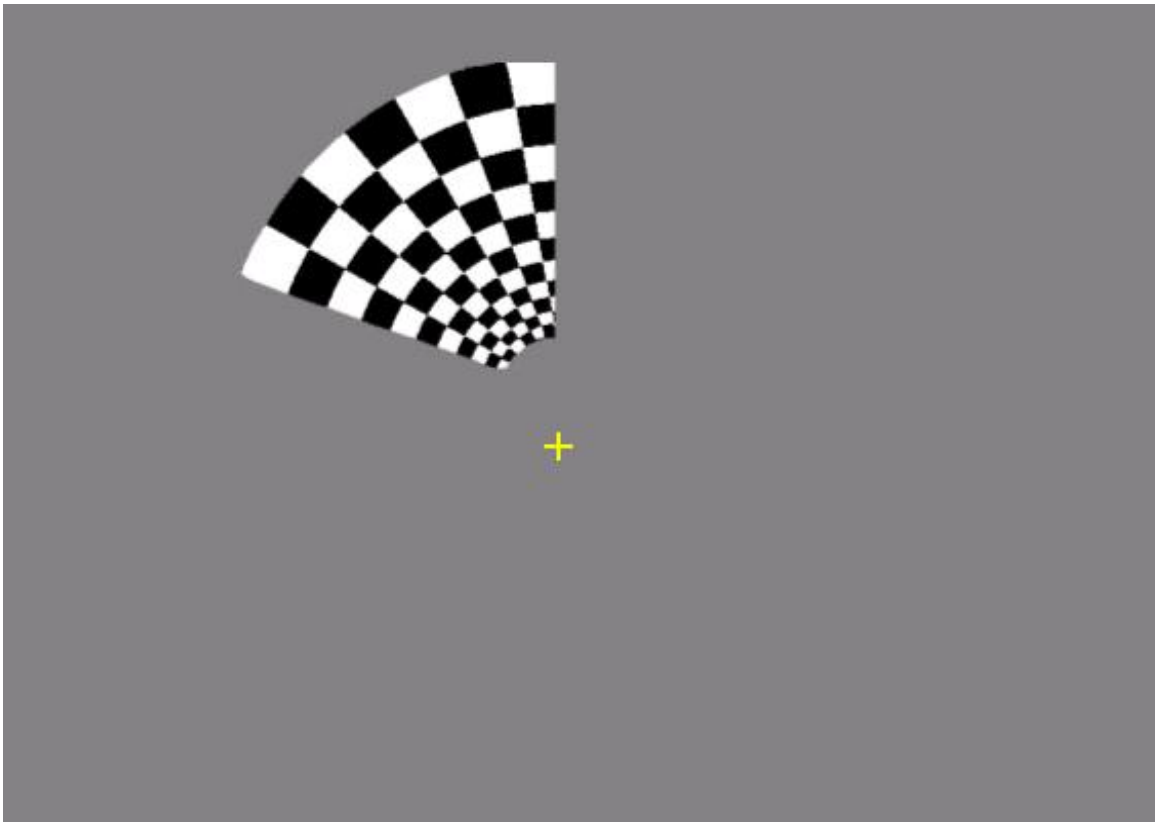

Figure 1. Left Upper Visual Field wedge checkerboard stimulus. A sixty degree black and white radial wedge image was used as visual stimuli to produce the retinotopic maps. The same radial wedge image was used for the four quadrants. The apex of the wedge faced the yellow crosshair and the adjacent side was aligned with the y coordinate axis for all 4 visual quadrant stimuli.

5. EEG Data Processing

The balistocardiogram artifact caused by blood flow pulsations in the brain and the MRI scanner pump and radiofrequency artifacts were corrected with post processing techniques. Biological artifacts from eye blinks, eye movements, and the electrocardiogram, were corrected offline also. Next, DC level correction and Global Field Power (GFP) were performed. With DC correction, the DC drifts caused by electrode charge buildup are removed and the application

of the GFP computes and applies a common reference to the data. For the ERP studies, data were filtered using a 200 Hz low pass value and a high pass value of 0.

In order to compute the SCPs, the time locked response to each 30 sec train of flashing checkerboard presentation was averaged for each quadrant. The group average file for each quadrant was used to perform the source reconstruction.

6. EEG Source Reconstruction

To accurately localize the source of the EEG activity measured, source reconstruction was performed. Both dipole fit and current density source reconstruction techniques were used. Boundary Element Model (6/8/9) was used as volume conductor. The boundary element method (BEM) calculates the electric potential of a current source by using triangulated brain compartments representing the brain, skull, and skin (Fuchs et al., 2002). For the simulated dipole fit a rotating dipole with 1 number of dipoles was selected. A Principal Component Analysis was used to get a regional dipole. For the sLORETA current density reconstruction, the M brain (female anatomical MRI brain) provided by Curry Source Localization software was selected. The M brain anatomical MRI is provided by Curry as a three dimensional image for the overlay of functional results. Skin was chosen for threshold segmentation and electrode positions for each study were imported and arranged in accordance with the 10-20 system. A baseline correction interval of -1 sec to 0 was selected. This same time interval was selected for noise estimation and Signal to Noise Ration measurements. The surface 21 brain template was selected to overlay EEG activity.

7. MRI Data Acquisition

Functional images were acquired with a 3 T Siemens Trio scanner. Images were acquired using a T2*-weighted gradient-echo, echo-planar imaging sequence with a repetition time (TR) of 2.0 sec and an echo time (TE) of 25 msecs. Thirty-four contiguous slices were collected with a voxel size of 4mm. Anatomical images were acquired using a T1-weighted sequence (TR = 500 msec, TE = 14 msec, FA = 90°, and voxel size of $0.94 \times 0.94 \times 5$ mm). Image processing was done using Statistical Parametric Mapping 5 (http://www.fil.ion.ucl.ac.uk/spm/). Anatomical scans were co-registered with their functional data.

8. fMRI Data Processing

Statistical Parametric Mapping (SPM) identifies neural regions activated during a particular task by making voxel (volumetric picture element) based statistical analysis using a standard statistical test to test hypotheses about functional imaging data. Statistical Parametric maps are under the null hypothesis are distributed according to a known probability density function, usually the Student's t or F distributions. This analysis can be performed within subjects or across subjects. During this process, the raw functional data is realigned by performing a 9 parameter affine transformation: x, y, z, coordinate translations, rotations, and scaling. Next, the data is spatially normalized into a template that conforms to a standard anatomical brain space. Afterwards, spatial smoothing of the data is performed. The main reason for smoothing is to render the errors more normal in their distribution to ensure the validity of inferences based on parametric tests. Next a General linear model is used to perform an analysis of covariance (Mazziota and Toga 1996).

C. EXPERIMENT 2

1. Subjects

Seven normal adult male volunteers were recruited from the local community and from the University of Texas at El Paso. The subjects ranged in age from 24 to 55 years, with a 40 year old mean. Subjects repeated the study up to 5 times with a minimum interval of one week between repetitions. All subjects gave informed consent before participating in accordance with the guidelines of the local Institutional Review Board (Appendix A).

2. EEG Subject Preparation

The subject preparation procedure was similar to Experiment 1.

3. EEG Recordings

EEG was recorded as in Experiment 1, except that the subjects sat in a chair 23 inches away from a 21 inch monitor in a comfortable position.

4. EEG Visual Stimulus Presentation

The same stimulus used in Experiment 1 was projected to a 21 inch color Dell Monitor at an approximate viewing distance of 50 cm. Visual stimuli consisted of a total of 10 repetitions of 30 sec block stimuli with 90 checkerboard presentations per train per quadrant.

5. EEG Data Processing

The electrical artifacts from eye blinks, eye movements, and the electrocardiogram, were corrected offline. For the ERP studies, data were filtered as in Experiment 1. For SCPs, data were filtered using a low pass filter of 4 Hz and a high pass filter value of 0.

In order to compute the VEPs, the time locked response to each presentation of the flashing checkerboard was averaged for each quadrant. An electrode of interest was selected for every visual field. This selection was based on the largest amplitude observed for each field (Figure 2). PO8 was selected as the electrode of interest for the Left Upper visual field stimuli, PO4 for the Left Lower, PO7 for the Right Upper, and PO3 for the Right Lower stimuli.

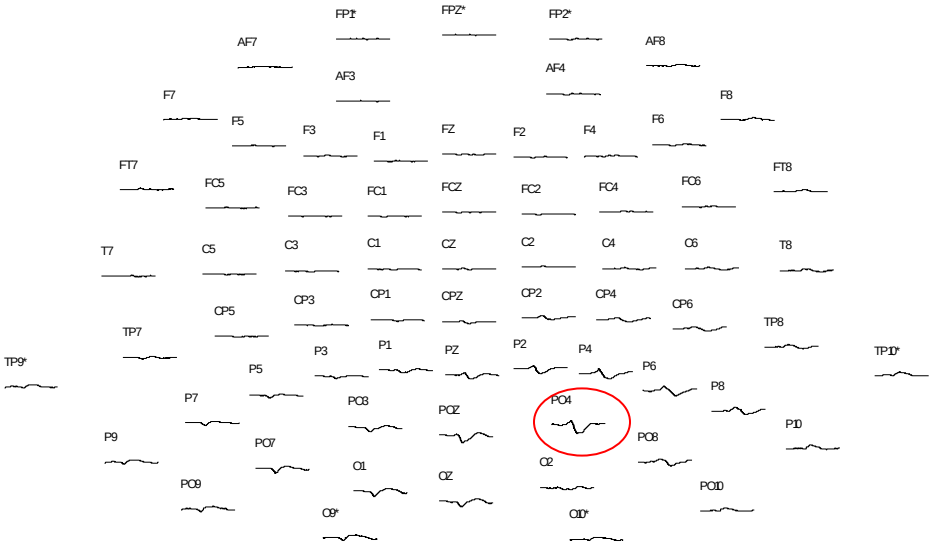

Figure 2. 10 Sec Left Lower Evoked Potential. The selection for the electrode of interest for each quadrant was based on the largest amplitude observed in the occipital area. Electrode PO4 was selected for the Left Lower evoked potential.

Amplitude and latency measurements were taken for P1, N1, and P2 waves (Figure 3), and One Way Analysis of Variance was performed. The P1 (or P100) wave is the large positive component of the VEP. It peaks at approximately 100 ms (Di Russo et al., 2005). The visual

N1 (or N100) wave is a large negative component. The N denotes its negative polarity and the 100 denotes the time of its peak which is at approximately 150 msecs. Its amplitude is reported to be modulated by visual attention (Luck et al., 2000). The P2 component of the VEP is the positive electrical potential which peaks at approximately 200 ms after the stimulus onset. Its amplitude has been reported to change with age (Crowley & Colrain, 2004). During this study, amplitude and latency measurements were taken for the electrodes of interest for each visual field for each of these components (Figure 3). . A One Way Analysis of Variance was performed on the amplitude measurements for the P1, N1, and P2 components (Figure 11).

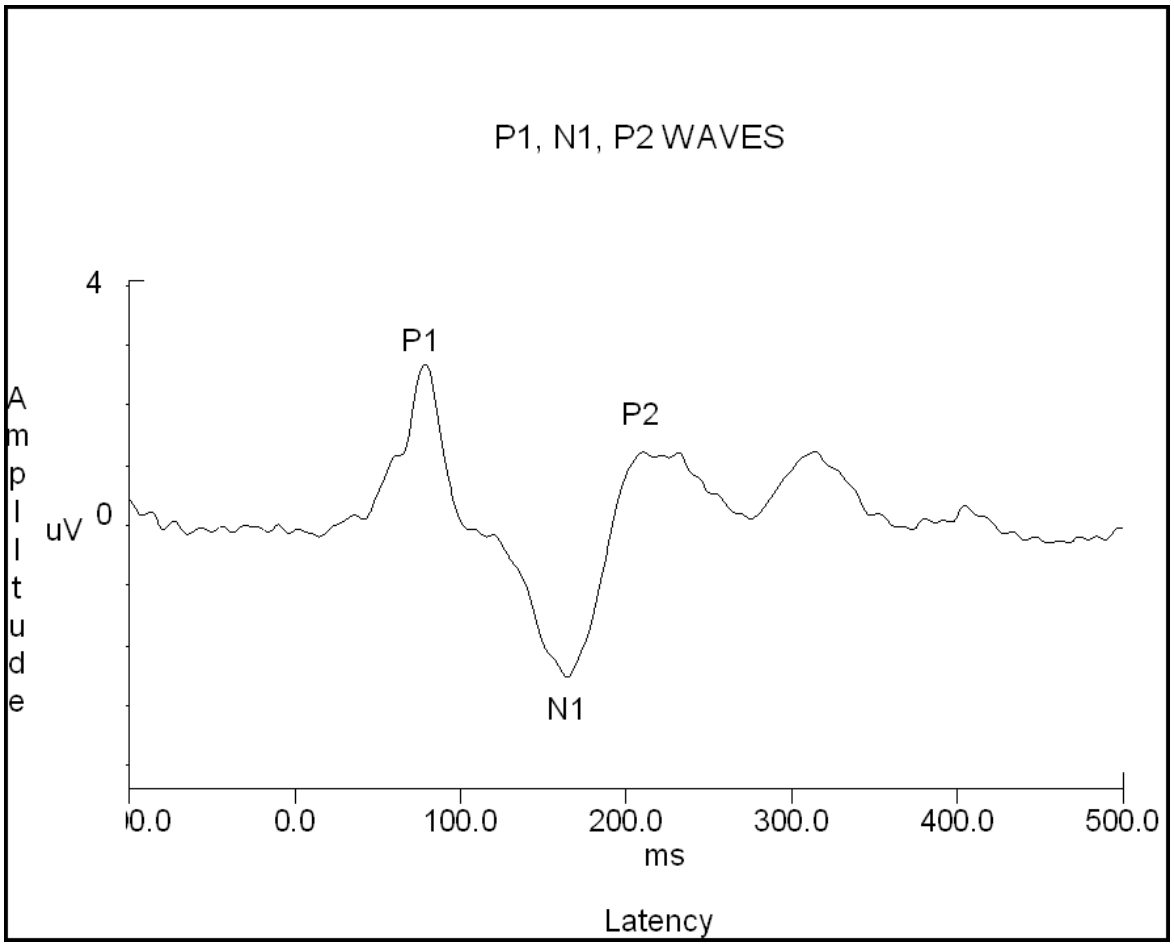

Figure 3. Representative Visual Evoked Potential. A typical VEP response to a flashing black and white checkerboard stimulus is shown for a single subject. The latency for the P1

wave occurs at approximately 100 ms after stimulus onset, while latencies are about 175 msec for N1 and 200 msec for the P2 components.

In order to compute the SCPs, the time locked response to each 30 sec train of flashing checkerboard presentation was averaged for each quadrant (Figure 4). The group average file for each quadrant was used to perform the source reconstruction.

D. EXPERIMENT 3

1. Subjects

Thirty-two healthy paid volunteers (25 male, 7 female; 29 right handed, 3 left handed) were recruited from the local community including the University of Texas at El Paso. Their ages ranged from 18-59 years, with a mean of 31.93 years. Their consent to participate in the study was obtained in accordance with the guidelines of the local Institutional Review Board (Appendix A).

2. EEG Subject Preparation.

The subject preparation procedure was similar to that in Experiments 1 and 2.

3. EEG Recordings

EEG recordings were made as in Experiment 2.

4. EEG Visual Stimulus Presentation

The same stimulus used in Experiment 1 was projected to a 21 inch color Dell Monitor at an approximate viewing distance of 50 centimeters. Visual stimuli consisted of a total of 10 repetitions of a 10 sec block stimuli with 30 checkerboard presentations per train per quadrant.

5. EEG Data Processing

EEG recordings were collected, corrected for biological and electrical artifacts, filtered, and analyzed as in Experiment 2. To compute the SCPs, the time locked response to each 10 sec train

of flashing checkerboard presentation was averaged for each quadrant (Figure 4). The group average file for each quadrant was used to perform the source reconstruction.

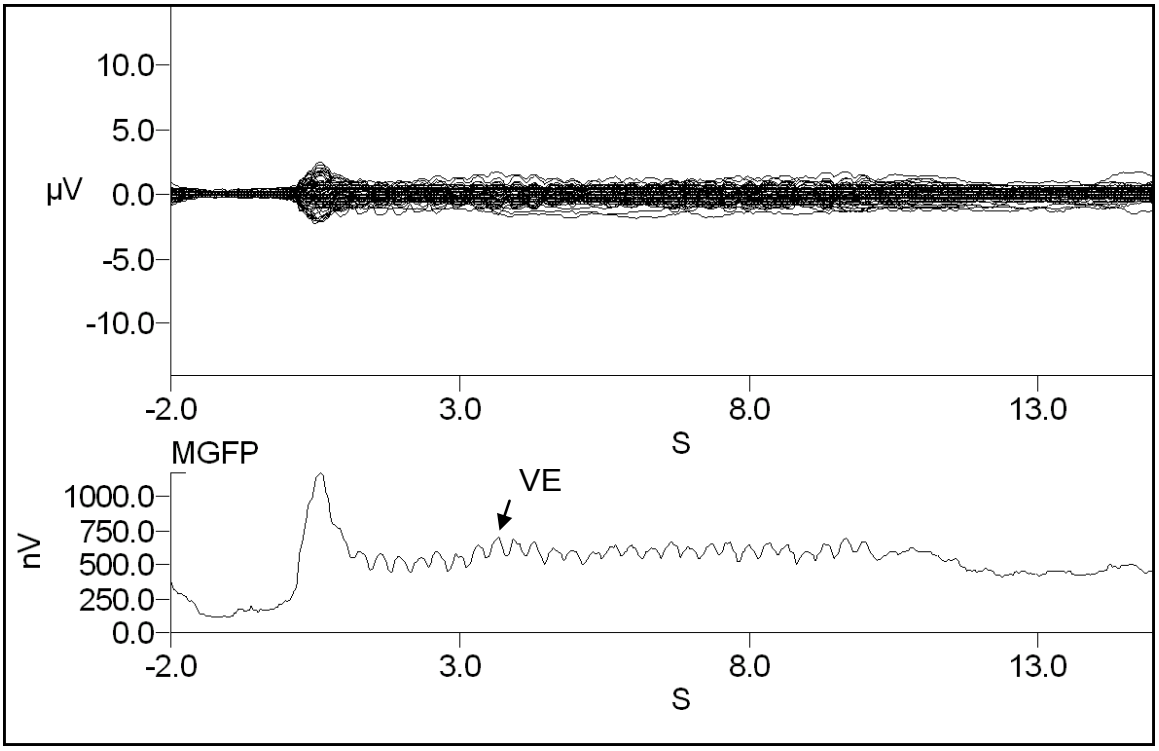

Figure 4. Slow Cortical Potentials. A representative butterfly plot of responses from all 68 channels to stimulus presentation in the Right Lower visual field is shown above the Mean Global Field Power (MGFP) plot in response to the same stimulus. The initial peak of neural activity can be seen in the MGFP plot at the onset of the stimuli; activity goes down but remains at approximately 500 nV and approximates zero by the end of the 10 sec stimuli. Activity takes time to return to baseline. VEPs can be observed as small bumps over the slow wave plot.

Global field power (GFP) quantifies the amount of activity at each time point. By measuring the area under the curve for the mean GFP, neural activity for each quadrant can be measured.

6. EEG Source Reconstruction

Source reconstruction was conducted as in Experiments 1.

Chapter 3

RESULTS

A. Simultaneous EEG/fMRI studies.

Simultaneous EEG/fMRI retinotopic maps of the four visual fields were generated. The BOLD fMRI analysis localized left upper visual field stimuli to the right hemisphere inferior occipital cortex where primary visual information is processed (Figure 5a). Responses to left lower stimuli were localized to the right hemisphere superior occipital cortex (Figure 5b). Right upper visual field stimuli localized to the left hemisphere inferior visual cortex (Figure 5c), and right lower visual field stimuli localized to the left hemisphere superior visual cortex (Figure 5d). Dipole localization was derived simultaneously from the 68 channels of the VEP response at the 90 sec time point for stimuli from the four quadrants of the visual field. Both BOLD data and source reconstruction from EEG data showed equivalent localization of responses for stimuli from the four quadrants of the visual field (Figure 5), and the localizations were consistent with the well established retinotopic maps.

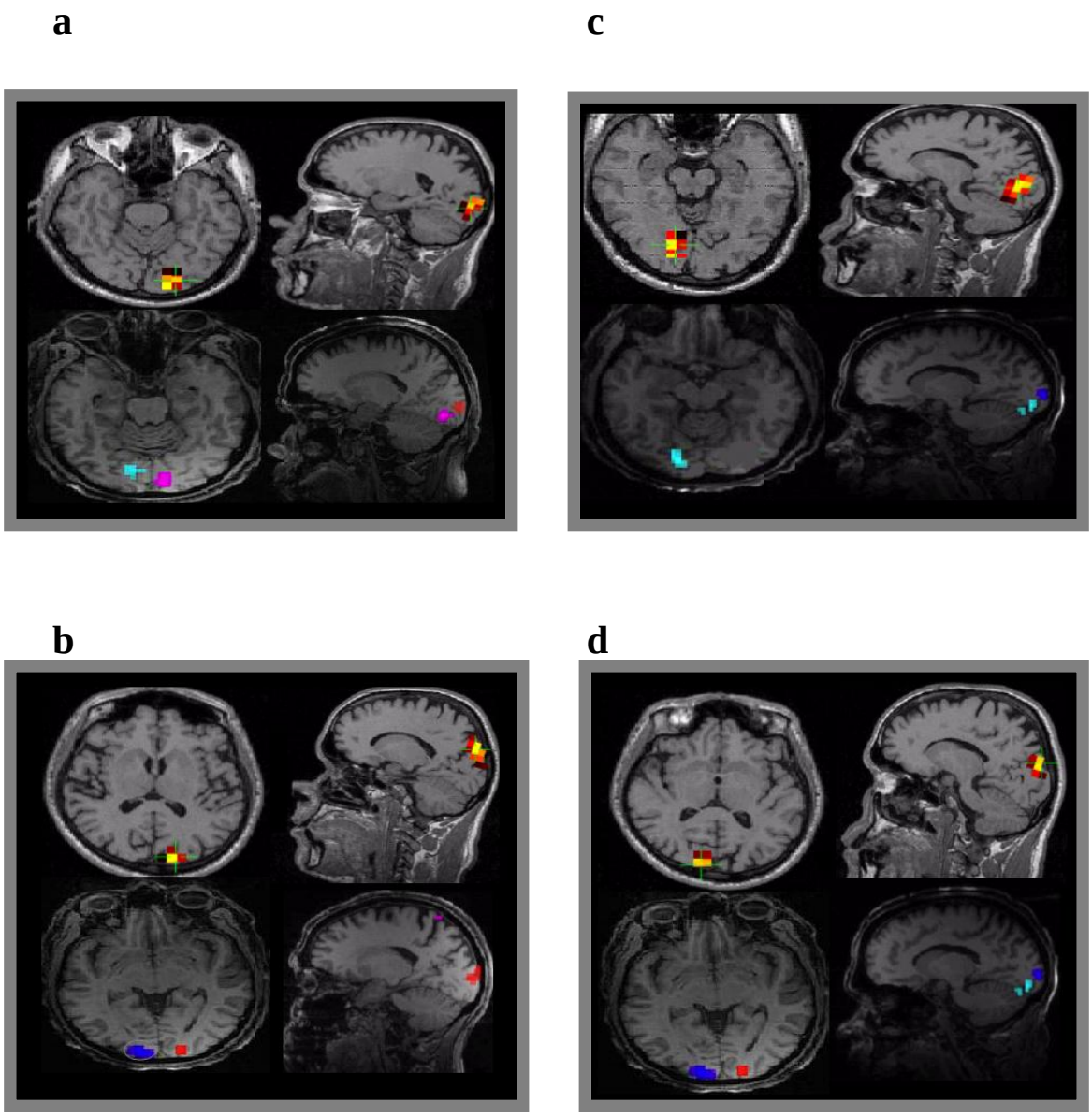

Figure 5. Retinotopic projection of visual stimuli to the cerebral cortex, assessed by BOLD responses and group dipole source analysis. Color-coded responses are overlaid on the female M anatomical brain template in both sagital and axial planes The BOLD responses to stimuli are coded by (a) magenta from the left upper quadrant, (b) red from the left lower quadrant, (c) cyan from the right upper quadrant, and (d) blue from the right lower quadrant, and overlaid on the subject's anatomical MRI with the group dipole response shown in brown, yellow, and orange.

Current Density Reconstruction of responses to stimuli from the four visual fields was also generated by sLORETA methodology. The EEG recordings used were collected simultaneously

with fMRI. Localization was derived from the 68 channels of the VEP response to the four quadrants of the visual field. All reconstructions were based on activity at 150 msecs. Left upper visual field stimuli again activated the right hemisphere inferior occipital cortex (Figure 6a), while left lower visual field stimuli localized to the right hemisphere inferior occipital cortex (Figure 6b), right upper visual field stimuli localized to the left hemisphere inferior visual cortex (Figure 6c), and right lower visual field stimuli localized to the left hemisphere superior visual cortex (Figure 6d). Thus, sLORETA current density maps also show consistent localizations with the well established retinotopic maps.

The sLORETA results divide each current by the size of its associated error bar, yielding F scores of activation (Appendix B). These calculations produce pseudo-statistics values which are only estimates of activity.

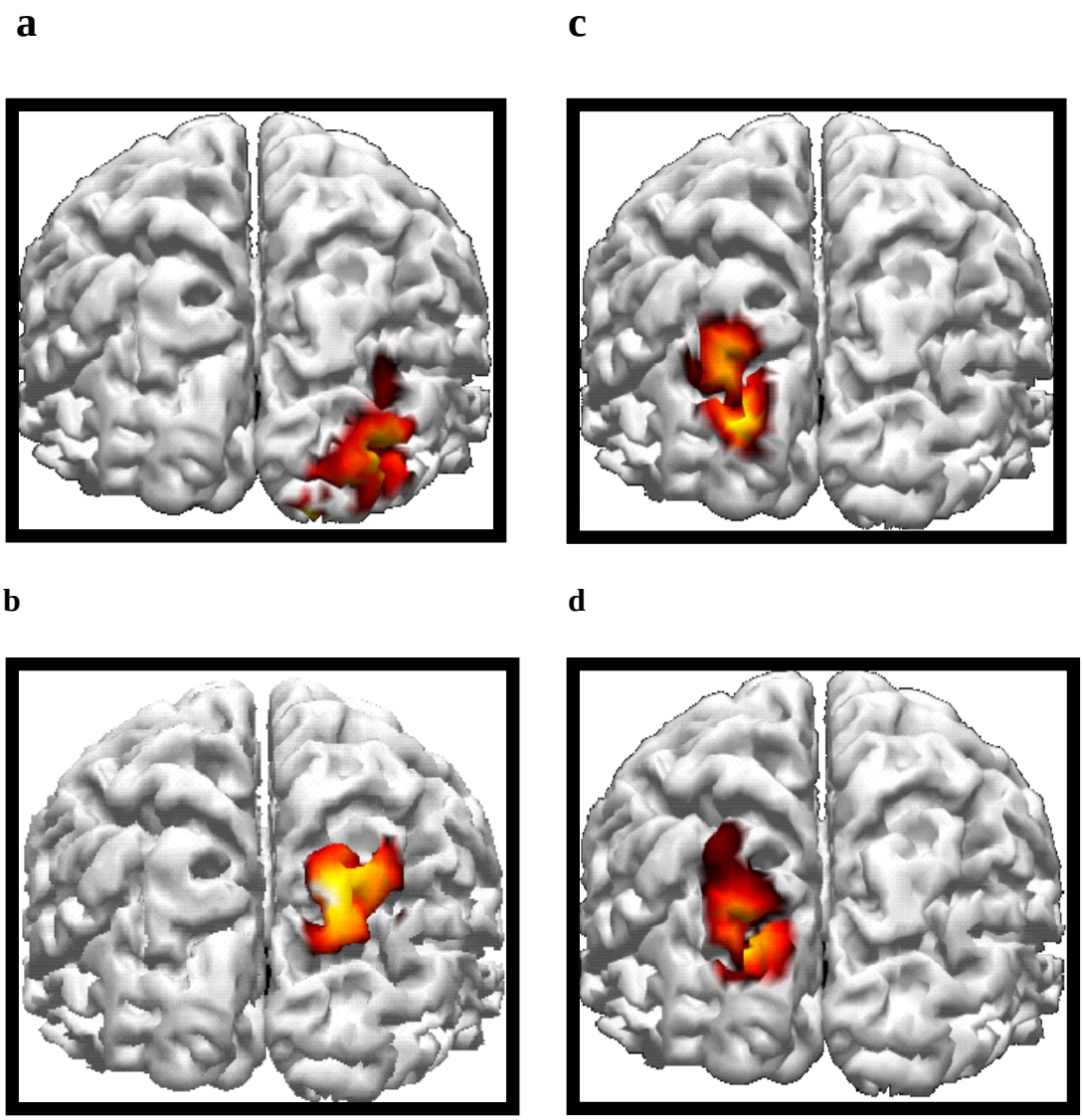

Figure 6. Current density reconstruction retinotopic maps by sLORETA analysis of EEG data. Responses were elicited from stimuli presented in the (a) left upper, (b) left lower, (c) right upper, or (d) right lower visual fields. Current density reconstruction is overlaid on the female M Anatomical brain template. F Distributed values ranged from 410 to 5484.

B. P1 Variability

The amplitude of the EEG signal varied for the same participant from one study to another. Four repetitions of the same experiment were performed with a minimum of one week between studies and the amplitude for the P1, N1, and P2 components were compared for the same

participant and same electrode. High variability was observed amongst studies in all 3 components. The P1 amplitude range was 0.78 to 1.87 uV with a mean of 1.16 and a Standard Error of the Mean value of 0.26. (Figure 7).

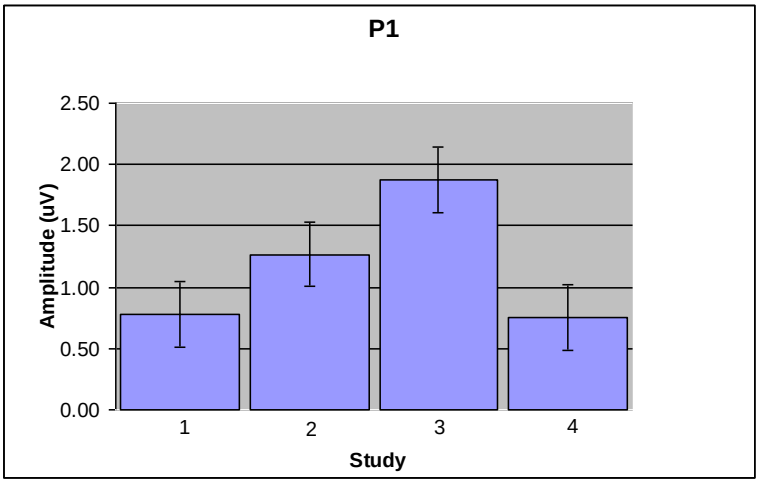

Figure 7. P1 amplitude and variance for the 30 second Left Upper Visual field study. The P1 amplitude for the same subject was determined from measurements on four different occasions.

The amplitude of the EEG signal also varied from subject to subject. The amplitude of the P1 wave for the 10 sec Upper Visual Field study was compared among 28 participants (Figure 8). A high degree of variability was observed. The P1 amplitude ranged from 1.2 to 8.9 uV with a mean of 3.58 and a Standard Error of the Mean of 0.36.

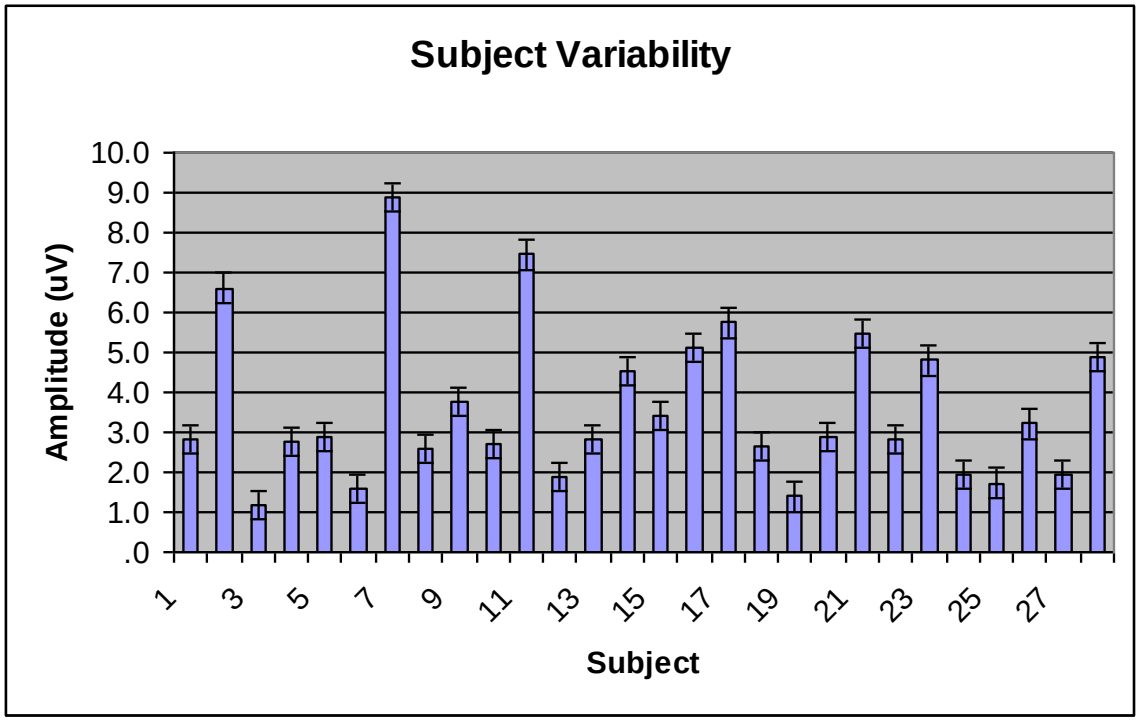

Figure 8. P1 amplitude variation among individuals in the 10 second Left Upper Visual field study. Data were collected from 28 different participants. The error bars represent the standard error of the mean.

To further investigate P1 variability, a One-Way ANOVA analysis to compare the intrasubject versus intersubject amplitude variability was conducted for the 30 second Experiment (Figure 9, ANOVA Table 1). No significant difference on amplitude was observed for either the intrasubject or intersubject groups. It is important to observe that the n value for all the groups was 3 and this factor may have an effect on these results.

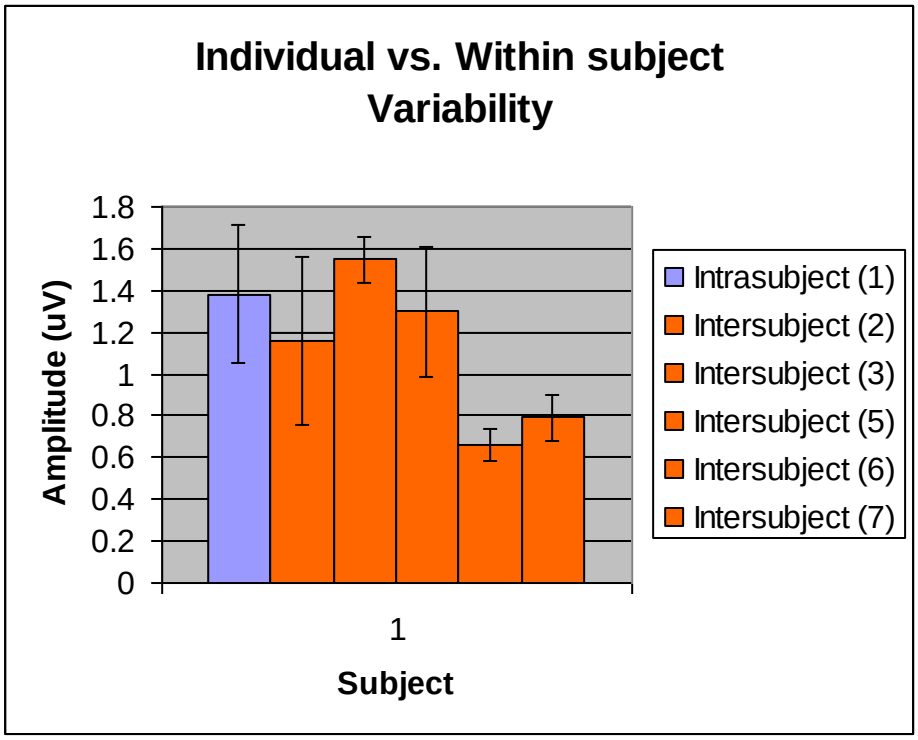

Figure 9. P1 amplitude variation amongst individuals and within individuals for the 30 second Left Upper Visual field study. Intrasubject data were collected from 3 different participants and repeated amplitude measurements were collected from 5 different participants. The error bars represent the standard error of the mean.

Table 1. P1 amplitude variation among individuals and within individuals for the 30 second Left Upper Visual field study. According to Table 1, the p value is > 0.05. Since we can not reject the null hypothesis there is no significant difference within the groups.

Individual vs. Within subject Amplitude variability One-Way ANOVA					
	Sum of Squares	df	Mean Square	F	Sig.
Between Groups	1.824	5	0.365	1.784	0.191
Within Groups	2.454	12	0.204		
Total	4.278	17			

C. Brain Activity for different stimulus duration and number of repetitions.

Global Field Power (GFP) analysis quantifies the amount of activity at each time point. By measuring the area under the curve for SCPs, the mean GFP can be measured as an indicator of neural activity for each quadrant (Figure 10). To compare brain activity between Experiment 2, which consisted of 10 repetitions of 30 sec train intervals with 90 stimuli per train, and Experiment 3, which consisted of 10 repetitions of 10 sec train intervals with 30 stimuli per train, a One-Way ANOVA was conducted. All visual fields of the 10 sec study presented very similar levels of activity. For the 30 sec study; more variability was observed for the 4 visual fields. A large brain activity difference was observed between the 2 groups.

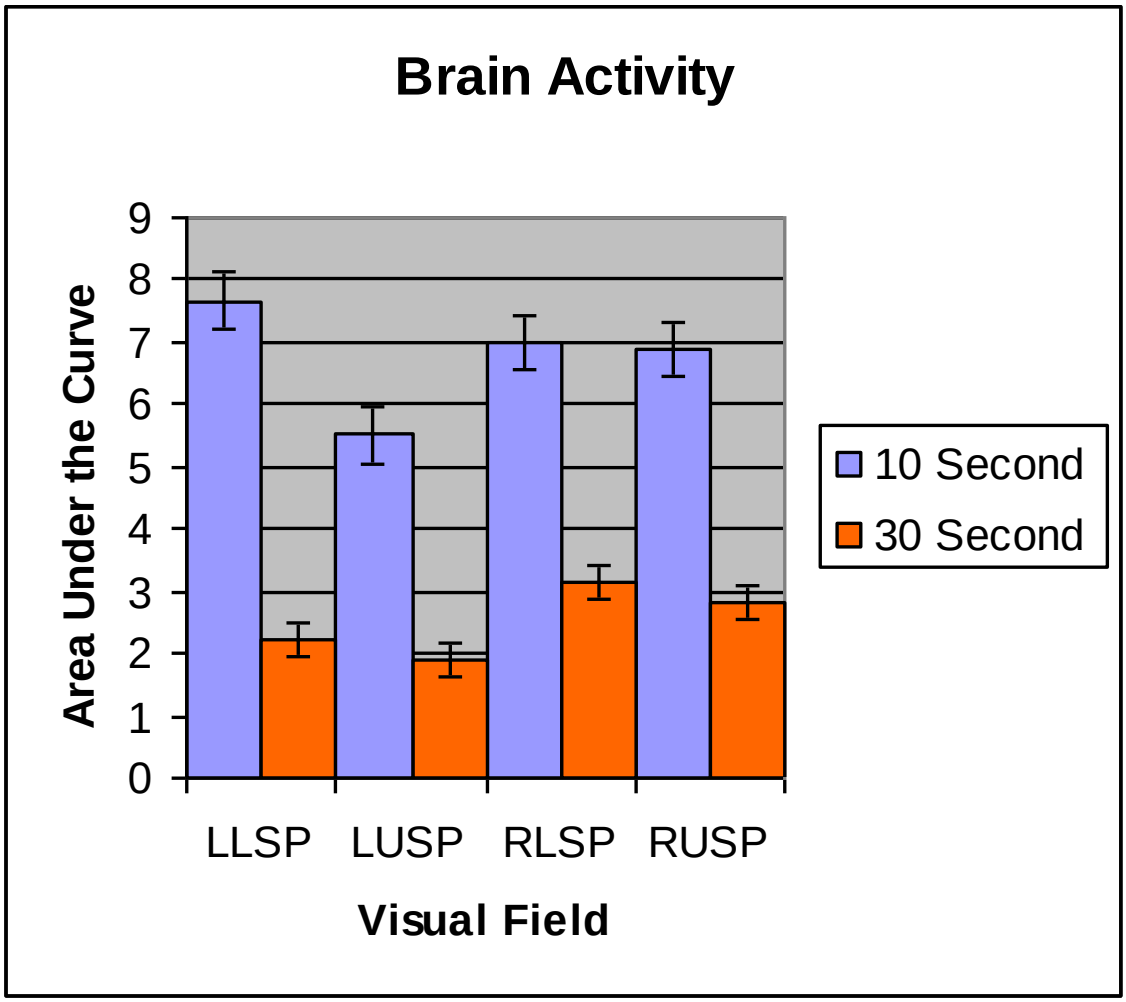

Figure 10. GFP analysis of brain activity for the 30 second (Experiment 2) and the 10 second (Experiment 3) studies. The F Score for a One-Way ANOVA at a significance level of 0.05 was 63.226 (Appendix B).

D. P1, N1, and P2 amplitude visual field variance

In Experiment 2, the amplitude of the P1 wave in response to stimuli from the lower quadrants was shown to be significantly larger than that from the upper quadrants by a One-Way ANOVA analysis (Figure 11, Table 2). A similar pattern was observed for the N1 lower components. For the P2 components, amplitude was lowest in response to stimuli from the upper left, and greatest in response to stimuli from the lower right. The smaller amplitude of P1

and N1 from upper field stimuli can be detected by simple visual inspection of the Evoked Potential (Figure 2).

The smaller amplitude for upper field components was also observed on Experiment 3 (Figure 12, Table 3), but the differences were significant only for the N1 and P2 components. These smaller amplitudes might be caused by a deeper location of primary visual cortex at the location of the PO8 (Left Upper stimulus) and PO7 (Right Upper stimulus) electrodes of interest.

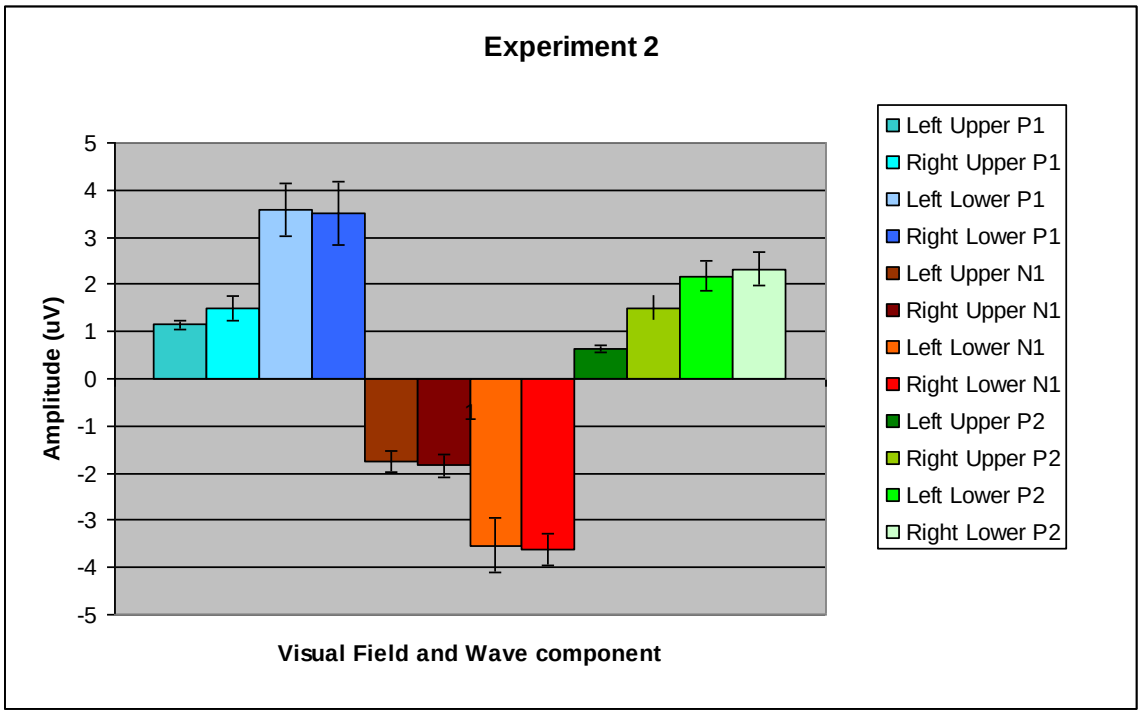

Figure 11. Amplitude and variance of P1, N1, and P2 waves in response to stimuli in different visual fields (Experiment 2). Bars represent the mean amplitude response to the different visual fields for each quadrant's electrode of interest (Left Opper_Electrode PO8, Left Lower_Electrode PO4, Right Upper_Electrode PO7, and Right Lower_Electrode PO3).

Table 2. Amplitude and variance of P1, N1, and P2 waves in response to stimuli in different visual fields (Experiment 2) ANOVA table.

Amplitude One-Way ANOVA Experiment 2				
			F	Sig.
Between Groups P1	(Combined)		7.311	0
	Linear Term	Weighted	1.216	0.274
		Deviation	10.358	0
Between Groups N1	(Combined)		6.488	0.001
	Linear Term	Weighted	0.195	0.661
		Deviation	9.635	0
Between Groups P2	(Combined)		4.572	0.006
	Linear Term	Weighted	2.013	0.161
		Deviation	5.851	0.005

Amplitude differences were detected among the electrode of interest for each visual field's P1, N1, and P2 wave, and a one- way Analysis of Variance was conducted at a 0.05 significance level. No significant difference was observed for the P1 component. For the N1 component, both left lower and right lower field's amplitude were more then twice the amplitude for both upper field components. A significant difference was observed in the Multiple Comparisons between Right Upper Visual field and Right Lower and Left Lower fields, Right Lower Visual Field and Right Upper and Left Upper, Left Lower Visual Field and Right Upper and Left Upper fields, and between Left Upper and Right Lower and Left Lower.

For the P2 components multiple comparisons, a significant difference was observed between Right Upper and Left Lower, Left Lower and Left Upper and Right Upper, Left Upper and Left Lower.

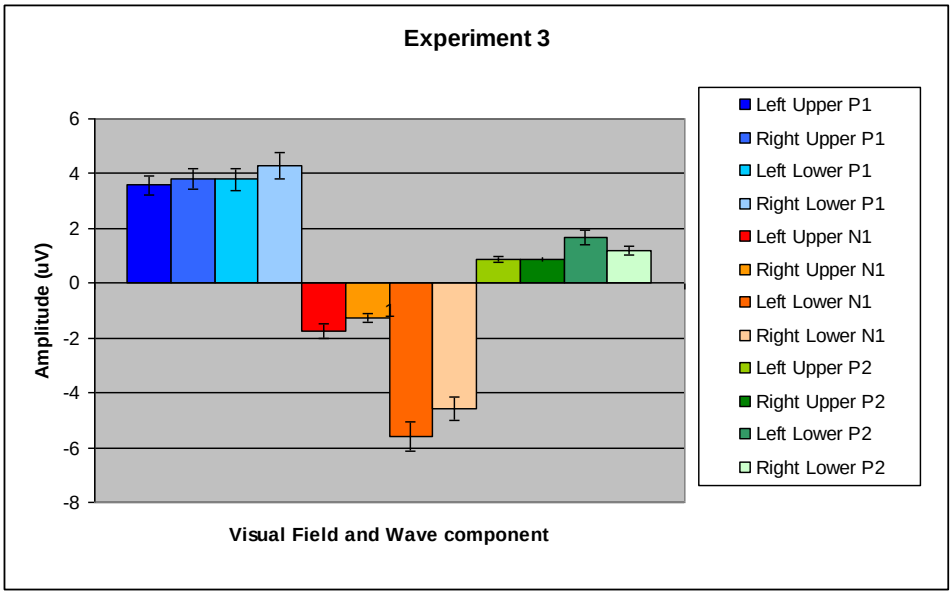

Figure 12. Amplitude and variance of P1, N1, and P2 waves in response to stimuli in different visual fields (Experiment 3). Bars represent the mean amplitude response to the different visual fields for each quadrant's electrode of interest (Left Opper_Electrode PO8, Left Lower_Electrode PO4, Right Upper_Electrode PO7, and Right Lower_Electrode PO3).

Table 3. Amplitude and variance of P1, N1, and P2 waves in response to stimuli in different visual fields (Experiment 3) ANOVA table.

Amplitude One-Way ANOVA Experiment 3				
			F	Sig.
Between Groups P1	(Combined)		0.835	0.478
	Linear Term	Weighted	0.819	0.368
		Deviation	0.842	0.434
Between Groups N1	(Combined)		27.382	0
	Linear Term	Weighted	2.502	0.117
		Deviation	39.822	0
Between Groups P2	(Combined)		4.676	0.004
	Linear Term	Weighted	0.811	0.37
		Deviation	6.609	0.002

E. Current Density Reconstruction of VEPs

Current Density Reconstruction of the four visual fields was generated (Figure 13). EEG localization was derived from the 68 channels of the VEP response to each of the four quadrants of the visual field. All reconstructions are displaying the activity at 150 msecs. Stimulus source localization analysis for the left lower visual field showed activation of right hemisphere superior occipital cortex, while left upper visual field stimuli showed localization to right hemisphere inferior occipital cortex, right upper visual field stimuli localized to left hemisphere inferior visual cortex, and right lower visual field stimuli localized to left hemisphere superior visual cortex. sLORETA current density maps show consistent localizations with the well established retinotopic maps.

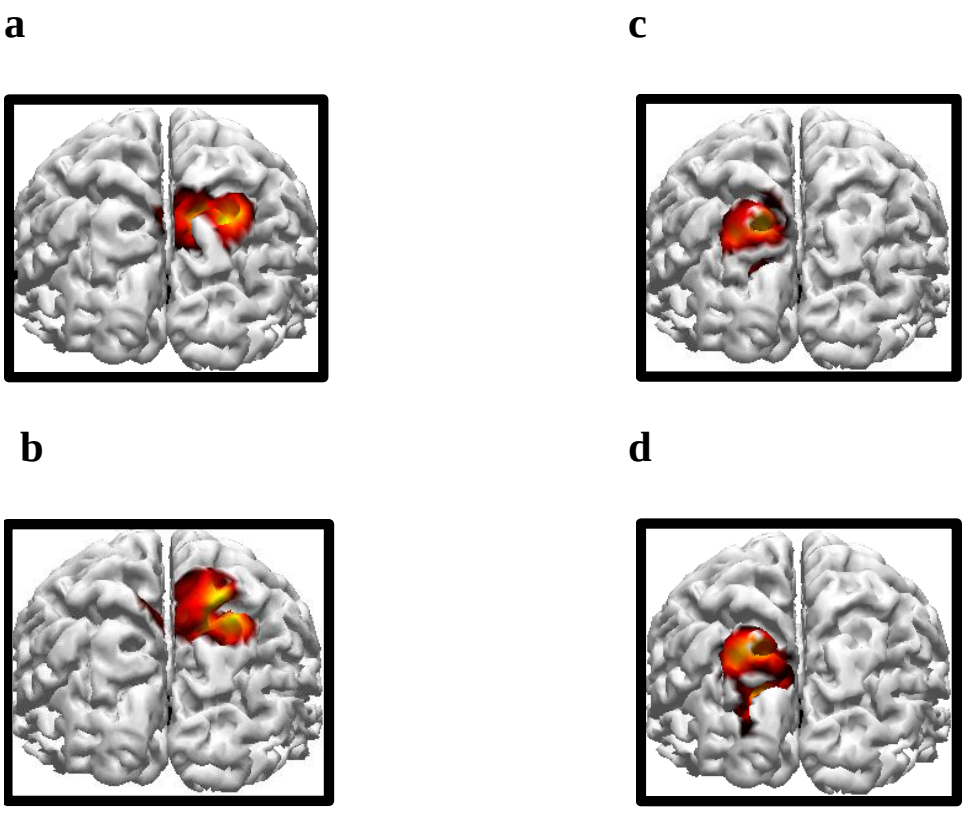

Figure 13. Current Density Reconstruction of Retinotopic VEPs. Responses were elicited from stimuli presented in the (a) left upper, (b) left lower, (c) right upper, or (d) right

lower visual fields. Current Density Reconstruction is overlaid on the female M Anatomical brain template. F Distributed values ranged from 725 to 11500 (Appendix B).

F. Current Density Reconstruction of SCPs

Current Density Reconstruction of the left lower (Figure 14), left upper (Figure 14), right lower (Figure 15), and right upper visual fields (Figure 15) were generated. EEG localization was derived from the 68 channels of the SCP response. In this case, reconstructions are displaying the activity at different points in time. Bilateral frontal and temporal activations were observed during the 10 secs of the source localization for all visual fields.

a **b**

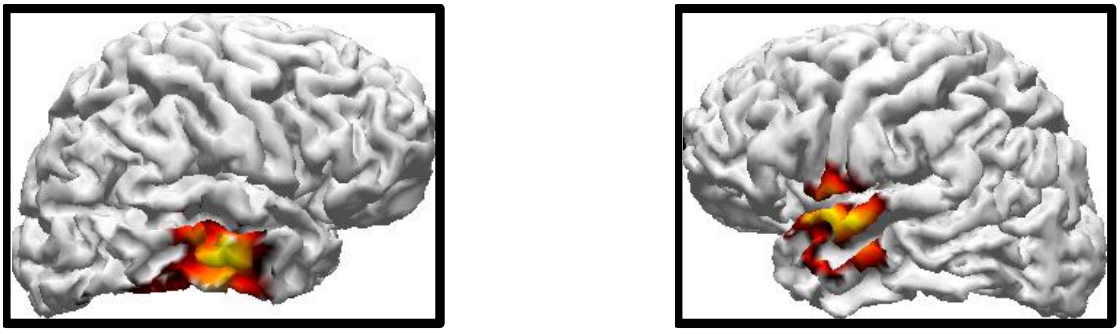

Figure 14. SCPs Current Density Reconstruction. Current Density Reconstruction is overlaid on the female M Anatomical brain template .

(a) Left Lower Visual Field stimuli showed activity at the left frontal lobe at 1,885 secs (CDR F Distributed Values Red 25,700 Yellow 36,805 (Appendix B)).

(b) Left Lower Visual Field stimuli showed activity at the right frontal lobe at 457 msecs (CDR F Distributed Values Red 11,000 Yellow 16,923 (Appendix B)).

a **b** **c**

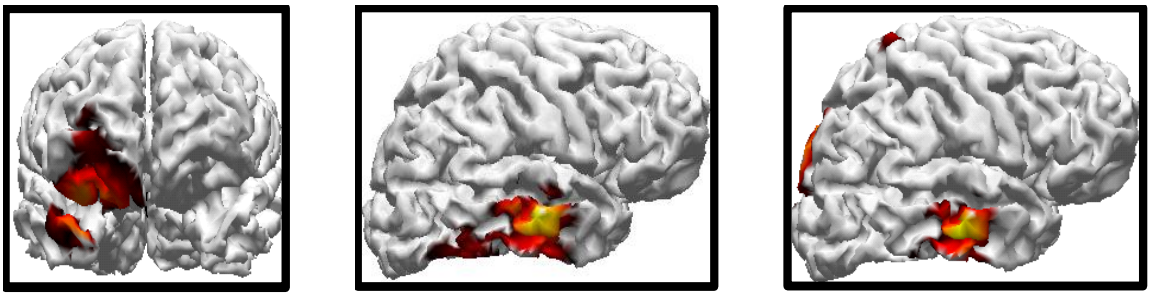

Figure 15. SCPs Current Density Reconstruction. Current Density Reconstruction is overlaid on the female M Anatomical brain template.

(a) Right Lower Visual Field stimuli showed activity at the right frontal lobe at 1,171 msecs (CDR F Distributed Values Red 9,300 Yellow 14,400 (Appendix B)).

(b) Right Lower Visual Field stimuli showed activity at the right temporal lobe at 6,685 msecs (CDR F Distributed Values Red 5,600 Yellow 8,600 (Appendix B)).

(c) Right Upper Visual Field stimuli showed activity at the right temporal lobe at 8,485 msecs (CDR F Distributed Values Red 13,371 Yellow 19,101 (Appendix B)).

Chapter 4

DISCUSSION

A. Equivalent localization for EEG and fMRI retinotopic maps

The BOLD response and the VEP dipole model source reconstruction retinotopic maps localization were consistent with retinotopic maps in the literature (Toga and Mazziotta, 2002). Left upper visual field stimuli showed primary visual cortex activation on the inferior right occipital cortex, left lower visual field stimuli showed primary visual cortex activation on the superior right occipital cortex, right upper visual field stimuli showed primary visual cortex activation on the inferior left occipital cortex, right lower visual field stimuli showed primary visual cortex activation on the inferior right occipital cortex. Mapping localization for the VEP dipole model was very similar to the fMRI localization. The sLORETA Current Density Reconstruction maps of the EEG data acquired in the simultaneous EEG/fMRI study were also consistent with the established retinotopic maps. It is worth mentioning and emphasizing that the EEG signal used for both the Dipole Model and sLORETA reconstructions was acquired simultaneously with the fMRI BOLD. It is important to emphasize that the acquisition of EEG in the harsh MRI scanner environment presents a big challenge since the radio frequency pulses and blood flow pulsation balistocardiogram artifacts contaminate the EEG signal. The current correction algorithms can clean most of the artifact but at the price of a small EEG signal degradation. The correct and coincident retinotopic maps obtained as a result of these experiments in spite of the challenges just mentioned are proof of the spatial accuracy that is provided by adequate source reconstruction techniques.

B. Amplitude variability of VEPs

Intrasubject and intersubject variability were also investigated during this study. The P1, N1, and P2 response to the Left Upper visual field was compared in 4 repeated studies of a single subject with a minimum time period of a week between repetitions.

Subject anatomical and functional variability of primary visual cortex as well as voltage distribution variability are reported by Dandekar et al. (2007). Calladay and Halliday (1973) provide evidence of decreased variability with age.

VEPs showed a high degree of intrasubject variability for all three P1, N1, and P2 components. When the amplitude of the P1 wave was compared across 28 participants, a high degree of intersubject variability was also observed (Figure 8). These results are an example of the sensitivity of the Evoked Potential studies, since they can detect amplitude differences within and between subjects. Since EEG sensitivity can detect minor changes in amplitude and latency, it can be applied to identify neurodegenerative disorders and the inclusion of the SCPs can provide additional information about the brain's functional connectivity.

Amplitude variability within and between subjects does not preclude our ability to use these visual evoked potentials to consistently localize the activity within the appropriate cortical region. Primary visual cortex functional and anatomical similarities are still prevalent and can be identified in retinotopic maps within and across subjects.

C. Neural activity and stimulus duration.

Neural activity for each visual field for both the 10 sec train duration and the 30 sec train duration was measured by computing the area under the curve of the MGFP. Activity was very similar for the four visual fields within each study but very different between studies. It was

interesting to observe increased activity with the shorter stimulus duration and shorter repetition of stimuli. This change might be caused by a decreased activity in the longer study caused by habituation to the visual stimuli.

D. Decreased P1 and N1 amplitude for upper hemifield stimulation

The smaller P1 and N1 upper fields' amplitude can be detected by simple visual inspection of the Evoked Potential Plot (similar to figure 2). This characteristic was not observed for the P2 wave. The smaller amplitude for upper field components was also observed in Experiment 3, but is only significant for the N1 component and not for the P1 component. This smaller amplitude might be caused by the deeper location of primary visual cortex involved in the processing of the upper hemifield.

E. EEG and SCPs, the answer to where and when

For the 10 sec train duration study which had VEPs and SCPs, a very clear retinotopic distribution can be observed for the VEP source reconstruction. Retinotopic representation is very similar to the one from the simultaneous EEG/fMRI. These results are an example of the detailed spatial information that can be determined by applying adequate source reconstruction techniques to EEG studies. The SCP source reconstruction provides detailed spatial information of frontal and temporal lobe activity as well as detailed temporal information for all activations in the msec range. These results are example of the combined spatial and temporal information on human brain function that can be obtained by taking advantage of the valuable information provided by the marriage of slow cortical potentials, Evoked Potentials, and source reconstruction.

F. SCPs and the brain's Default Mode Network

The combination of SCP data with source reconstruction, revealed neural activity associated with visual attention and vigilance in both temporal and frontal lobes. These results show how traditional EEG methods overlook major components of brain activity by filtering SCPs. The importance of this signal as a mapping tool for understanding the default mode brain activity during no task has recently been expressed by Raichle (2009). It has been proposed that SCPs, and possibly BOLD fluctuations in oxygenation, represent fluctuations in cortical excitability serving an important coordinating role in the integration of functional activity (Raichle, 2010). Schroeder and Lakatos (2009), view this as one mode of attention shift to match the predictable patterns of incoming information which results in enhanced response and improved performance. As described by Raichle, the brain default network is on cue, and when a novel or unpredictable event occurs, SCPs become temporarily suppressed. This suppression can explain the reduction in BOLD response to Default Mode Network areas and the increased activity in brain areas associated with goal-directed attention (Raichle, 2009). The current functional neuroimaging approach assumes the brain to be primarily reflexive but brain energy consumption points us in a different direction. If the brain is primarily reflexive, why is so much of its energy devoted to the ongoing intrinsic activity? The application of the full band EEG including the SCPs can provide an answer to this complicated question. SCPs can be used to study ongoing spontaneous activity. If this is the case, SCPs can provide a window on how the brain matches its predictions to cope with changing environmental demands. The relationship between Local Field Potentials and BOLD make SCPs the method of choice to better understand the spontaneous bold fluctuations (0.01-4 Hz) and the DMN.

G. Significance and Applications

The temporal resolution of EEG reflects the physiological rate of neuronal firing; and its spatial resolution – obtained from a large number of electrodes and in combination with source reconstruction -- can accurately map the source of that neural activity. It is non invasive, affordable, and can be performed in any setting. All of these characteristics expand the utility of the EEG to a large number of possible applications. The following paragraphs list only a few of them.

1. Neurocognitive Applications

a. Connectivity

SCPs and EEG source reconstruction may prove to be extremely valuable for connectivity analysis. The main purpose of connectivity studies is to identify regions in the brain which are functionally connected. The temporal information on the chronology of neural activity and the location of the different brain activity areas provided by these methods can be essential for connectivity studies.

b. BOLD response correlation

To further the understanding of the BOLD response, EEG can provide the temporal detail information for fMRI studies while SCPs can help capture the essence of the BOLD neural activity substrate.

c. The Default Mode Network

The importance of understanding the brain's Default Mode Network, or intrinsic pattern of activity, has previously been noted. The research described here demonstrates the great utility of EEG, as a more portable and user-friendly technique, for studying the human brain's intrinsic activity in its daily living scenario through SCPs and EEG source reconstruction. Understanding the brain's intrinsic activity patterns is essential for deciphering how the normal brain works.

d. Sensory studies

In this research, the neural activity response to flashing checkerboard stimuli was revealed in spatial and temporal detail in the visual system. In so doing, this work provides proof-of-concept for applying this technology to the study other sensory modalities, like somatosenory function, pain, and motor planning.

e. The neurophysiology of learning

Since it is painless and portable, it can be used to study the natural course of learning in infant populations in the classroom and help innovate teaching methods. Given that it can identify individual differences, it can also be applied to have a more tailored individual approach to teaching children with learning disabilities.

2. Clinical Applications.

a. Epilepsy

EEG recordings are currently used to localize the source of epileptic spikes for pre-surgical planning and some times, this information is not enough. The additional details that can be

provided by incorporating SCPs and source reconstruction to identify the areas affected or connected with the epileptic foci can have a big impact on pre-surgical mapping and epileptic surgery outcome.

b. Brain Injury, brain plasticity and neurogenesis.

Banking on its portability, SCP and EEG can be used in areas which lack more sophisticated imaging equipment to identify brain injury, to observe plastic changes during treatment, and to assess the progress of neurorehabilitation.

c. Attention deficit

SCPs open a window to the study of attention. It can be the ideal technique for studying attention in kids and the effects of the impact of modern current life styles on attention deficit and hyperactivity. A better understanding of these problems and its causes can have an effect on their diagnosis and treatment plans as well as the cure success rate.

3. Summary

EEG, SCPs, and source localization have endless future applications for research and clinical assessment of brain function and mental processes. The impact of a safe, painless, affordable, and portable imaging technique which has the ability to localize information processing in real time in the brain provides great potential for the assessment and treatment of neural deficits, and the improvement of our quality of life.

Chapter 5

CONCLUSION

The objective of this study was to conduct a thorough evaluation of EEG as an imaging tool. Retinotopic maps were created for each quadrant of the visual field by presenting a visual stimulus to each of the four visual quadrants. By combining Slow Cortical Potentials (SCPs) with Event Related Potentials (ERPs) and accurate source localization techniques, I was able to obtain spatial resolution equivalent to that achieved with fMRI, which is the mainstay neuroimaging technique because of its spatial localization. The VEP and SCP results on visual system retinotopy coincided with BOLD response retinotopic maps which were acquired simultaneously with EEG and also with the well established retinotopic maps in the literature.

The certainty and validity of brain imaging studies is more eminent when different modalities are validated by converging evidence. During this study, converging evidence resulted in equivalent retinotopic maps generated by combing EEG and fMRI. The activations found for the four visual fields with EEG source reconstruction overlap with the activations observed in the fMRI study without a doubt (Figure 5). Even though converging evidence is the most common method for multimodality brain imaging data fusion (Horowitz & Poeppel, 2002) , meta-analyses of data transformed into a cannoncial coordinate system and the application of spatial correlation analysis between fMRI and EEG data will be used for future studies to evaluate the extent of agreement across studies.

This study illustrates the usefulness and accuracy of sLORETA as a source reconstruction technique. Accurate spatial and temporal information on brain visual processing can be achieved by employing sLORETA source reconstruction on VEPs generated with visual stimuli.

This application of EEG to localize where and when a neural process is taking place is not limited to vision. It can be applied to study almost any brain activity. At the present time, EEG cannot achieve the sub-millimeter spatial resolution provided by fMRI but it can provide equivalent localization with the added advantages of (a) temporal resolution in the msec scale, (b) portability, (c) lack of discomfort associated with data acquisition, and (d) affordability. All of these advantages make EEG and SCPs an appropriate and effective method for studying and understanding the human brain and its neurological disorders.

References

Bangert M, Altenmuller E. 2003. Mapping perception to action in piano practice: a longitudinal DC-EEG study. BMC Neuroscience 4: 26.

Basile LFH, Brunetti EP, Pereira JJF, Ballester G, Amaro JE, Anghinah R, Ribeiro P, Piedade R, Gattaz WF. 2006. Complex slow potential generators in a simplified attention paradigm. International Journal of Psychophysiology 61: 149-157.

Birbaumer N. 1999. slow Cortical Potentials: Plasticity, Operant Control, and Behavioral Effects. The Neuroscientist 5: 74-78.

Braitenberg V, Schuz A. 1991. Anatomy of th eCortex: Statistics and Geometry. Anatomy of th eCortex: Statistics and Geometry. New York: Springer-Berlag.

Callaway E, Halliday RA. 1973. Evoked potential variability: Effects of age, amplitude and methods of measurement. Electroencephalography and clinical neurophysiology 34: 125-133.

Conway MA, Pleydell-Pearce CW, Whitecross SE. 2001. The Neuroanatomy of Autobiographical Memory: A Slow Cortical Potential Study of Autobiographical Memory Retrieval. Journal of Memory and Language 45: 493-524.

Crowley KE, Colrain IM. 2004. A review of the evidence for P2 being an independent component process: age, sleep and modality. Clinical Neurophysiology 115: 732-744.

Cui RQ, Egkher A, Huter D, Lang W, Lindinger G, Deecke L. 2000. High resolution spatiotemporal analysis of the contingent negative variation in simple or complex motor tasks and a non-motor task. Clinical Neurophysiology 111: 1847-1859.

Dandekar S, Ales J, Carney T, Klein SA. 2007. Methods for quantifying intra- and inter-subject variability of evoked potential data applied to the multifocal visual evoked potential. Journal of Neuroscience Methods 165: 270-286.

DeYoe EA, Bandettini P, Neitz J, Miller D, Winans P. 1994. Functional magnetic resonance imaging (FMRI) of the human brain. Journal of Neuroscience Methods 54: 171-187.

Di Russo F, Pitzalis S, Spitoni G, Aprile T, Patria F, Spinelli D, Hillyard SA. 2005. Identification of the neural sources of the pattern-reversal VEP. NeuroImage 24: 874-886.

Fischgold H. 1962. A history of the electrical activity of the brain, the first half-century: Mary A. B. Brazier (Pitman, London and Macmillan, New York, 1961, 119 p., 41 illus., 25 /- and $4.50). Electroencephalography and clinical neurophysiology 14: 968-969.

Fuchs M, Kastner J, Wagner M, Hawes S, Ebersole JS. 2002. A standardized boundary element method volume conductor model. Clinical Neurophysiology 113: 702-712.

He BJ, Raichle ME. 2009. The fMRI signal, slow cortical potential and consciousness. Trends in Cognitive Sciences 13: 302-309.

Heil M, Rösler F, Hennighausen E. 1997. Topography of brain electrical activity dissociates the retrieval of spatial versus verbal information from episodic long-term memory in humans. Neuroscience Letters 222: 45-48.

Hennighausen E, Heil M, Rösler F. 1993. A correction method for DC drift artifacts. Electroencephalography and clinical neurophysiology 86: 199-204.

Hiroshi S, Mark H. 2006. What is the Bereitschaftspotential? Clinical neurophysiology : official journal of the International Federation of Clinical Neurophysiology 117: 2341-2356.

Horwitz B, Poeppel D. 2002. How can EEG/MEG and fMRI/PET data be combined? Human Brain Mapping 17: 1-3.

Jost K, Beinhoff U, Hennighausen E, Rösler F. 2004. Facts, rules, and strategies in single-digit multiplication: evidence from event-related brain potentials. Cognitive Brain Research 20: 183-193.

Khader P, Heil M, Rösler F. 2005. Material-specific long-term memory representations of faces and spatial positions: Evidence from slow event-related brain potentials. Neuropsychologia 43: 2109-2124.

Khader P, Schicke T, Röder B, Rösler F. 2008. On the relationship between slow cortical potentials and BOLD signal changes in humans. International Journal of Psychophysiology 67: 252-261.

Khader P, Burke M, Bien S, Ranganath C, Rösler F. 2005. Content-specific activation during associative long-term memory retrieval. NeuroImage 27: 805-816.

Kriegseis A, Hennighausen E, Rösler F, Röder B. 2006. Reduced EEG alpha activity over parieto-occipital brain areas in congenitally blind adults. Clinical Neurophysiology 117: 1560-1573.

Lakatos P, Shah AS, Knuth KH, Ulbert I, Karmos G, Schroeder CE. 2005. An Oscillatory Hierarchy Controlling Neuronal Excitability and Stimulus Processing in the Auditory Cortex. J Neurophysiol 94: 1904-1911.

Logothetis NK, Pauls J, Augath M, Trinath T, Oeltermann A. 2001. Neurophysiological investigation of the basis of the fMRI signal. Nature 412: 150-157.

Luck SJ, Woodman GF, Vogel EK. 2000. Event-related potential studies of attention. Trends in Cognitive Sciences 4: 432-440.

Malmivuo J. 2005. The relative merits of EEG and MEG. Proc. Estonian Acad. Sci. Eng. 11: 69-82.

Menon V, CrottazHerbette S. 2005. Combined EEG and fMRI Studies of Human Brain Function. Pages 291-321 in Michael FG, ed. International Review of Neurobiology, vol. Volume 66 Academic Press.

Millett D. 2001. Hans Berger from psychic energy to the EEG. Perspectives in Biology and Medicine 44: 522-542.

Müller NG, Mollenhauer M, Rösler A, Kleinschmidt A. 2005. The attentional field has a Mexican hat distribution. Vision Research 45: 1129-1137.

Ogawa S, Menon RS, S.G. K, Gerbil K. 1998. ON THE CHARACTERISTICS OF FUNCTIONAL MAGNETIC RESONANCE IMAGING OF THE BRAIN. Annu. Rev. Biophys. Biomol. Struct. 27: 447-474.

Oostenveld R, Praamstra P. 2001. The five percent electrode system for high-resolution EEG and ERP measurements. Clinical Neurophysiology 112: 713-719.

Pascual-Marqui RD. 2002. Standardized low resolution brain electromagnetic tomography (sLORETA): technical details. Methods & Findings in Experimental & Clinical Pharmacology 24D: 5-12.

Posner MI, Raichle ME. 1998. Images of mind. Images of Mind.

Raichle ME. 2010. Two views of brain function. Trends in Cognitive Sciences 14: 180-190.

Raichle ME, Snyder AZ. 2009. Intrinsic Brain Activity and Consciousness. Pages 79-88 in Steven L, Giulio T, eds. The Neurology of Consciousness. San Diego: Academic Press.

Rolke B, Heil M, Hennighausen E, Häussler C, Rösler F. 2000. Topography of brain electrical activity dissociates the sequential order transformation of verbal versus spatial information in humans. Neuroscience Letters 282: 81-84.

Rösler F, Heil M, Röder B. 1997. Slow negative brain potentials as reflections of specific modular resources of cognition. Biological Psychology 45: 109-141.

Rösler F, Röder B, Heil M, Hennighausen E. 1993. Topographic differences of slow event-related brain potentials in blind and sighted adult human subjects during haptic mental rotation. Cognitive Brain Research 1: 145-159.

Scherg M. 1990. Fundamentals of Dipole Source Potential Analysis. Advances in Audiology 1990: 40-69.

Schroeder CE, Lakatos P. 2009. Low-frequency neuronal oscillations as instruments of sensory selection. Trends in Neurosciences 32: 9-18.

Sossi V. 2003. Positron emission tomography (PET) advances in neurological applications. Nuclear Instruments and Methods in Physics Research Section A: Accelerators, Spectrometers, Detectors and Associated Equipment 510: 107-115.

Strehl U, Leins U, Goth G, Klinger C, Hinterberger T, Birbaumer N. 2006. Self-regulation of Slow Cortical Potentials: A New Treatment for Children With Attention-Deficit/Hyperactivity Disorder. Pediatrics 118: e1530-1540.

Thordstein M, Flisberg A, Löfgren N, Bågenholm R, Lindecrantz K, Wallin BG, Kjellmer I. 2004. Spectral analysis of burst periods in EEG from healthy and post-asphyctic full-term neonates. Clinical Neurophysiology 115: 2461-2466.

Toga AW, Mazziotta JC. 2002. Introduction to Cartography of the Brain in Arthur WT, John CM, eds. Brain Mapping: The Methods (Second Edition). San Diego: Academic Press.

Vanhatalo S, Voipio J, Kaila K. 2005. Full-band EEG (FbEEG): an emerging standard in electroencephalography. Clinical Neurophysiology 116: 1-8.

Vanhatalo S, Tallgren P, Andersson S, Sainio K, Voipio J, Kaila K. 2002. DC-EEG discloses prominent, very slow activity patterns during sleep in preterm infants. Clinical Neurophysiology 113: 1822-1825.

Walter WG, Cooper R, Aldridge VJ, McCallum WC, Winter AL. 1964. Contingent Negative Variation : An Electric Sign of Sensori-Motor Association and Expectancy in the Human Brain. Nature 203: 380-384.

Appendix A

Study Number _____

HUMAN SUBJECTS CONSENT FORM

The following is a brief summary of the project in which you are asked to participate. Please read this information before signing the statement below.

TITLE OF PROJECT: EEG slow potentials during visual processing and learning.

PURPOSE OF STUDY/PROJECT: To study the EEG response to visual processing, attention, and learning. Eye tracking will be also be recorded during this studies.

PROCEDURE: Conductive electrodes will be placed in your hair to record your brain activity. A conductive gel/electrolyte will be used to attach each electrode to your head. You will be asked to view videos while wearing the electrodes.

INSTRUMENTS: An EEG (electroencephalogram) amplifier will be used to amplify and record your brain activity. Your eye movements will be recorded with the aid of a goggle mounted camera.

BENEFITS/COMPENSATION: $15 Per hour

I, _____, attest with my signature that I have read and understood the following description of the study, "Slow potentials during visual processing and learning", and its purposes and methods. I understand that my participation in this research is completely voluntary and my participation or refusal to participate in this study will not affect my relationship with Sand's Research in any way. Further, I understand that I may withdraw at any time or refuse to answer any questions without penalty. Upon completion of the study, I understand that the results will be freely available to me upon request. I understand that the results of my survey will be confidential, accessible only to the principal investigators, myself, or a legally appointed representative. I have not been requested to waive nor do I waive any of my rights related to participating in this study. I understand that there are no risks associated with an EEG study.

If I need to talk to someone about my experience during this experiment, I can call Karen Hoover, IRB Administrator at the University of Texas at El Paso Institutional Review Board, (915) 747-7939 or Ph.D. Stephen F. Sands, President of Sands Research, (915) 760-5253.

I understand that I can ask for a copy of this form. I have read and understand the above.

_____ _____

Signature of Participant **Date**

_____ _____

Signature of Experimenter **Date**

Appendix B

FIUGRE 5. Current Density Source Reconstruction F values

a. Left Upper

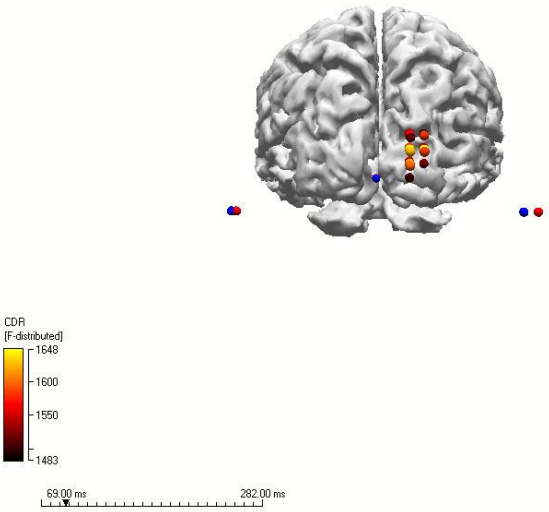

b. Left Lower

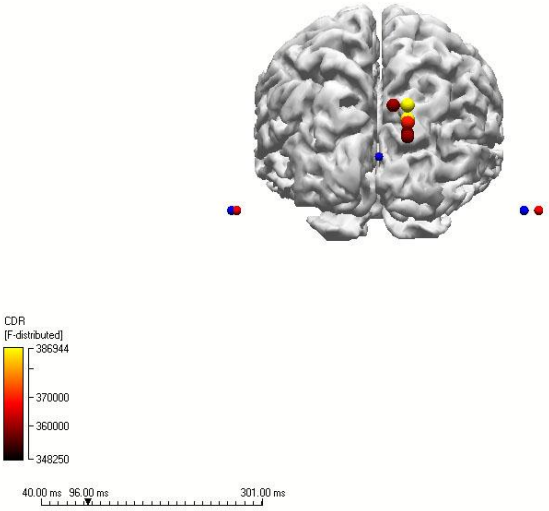

c. Right Upper

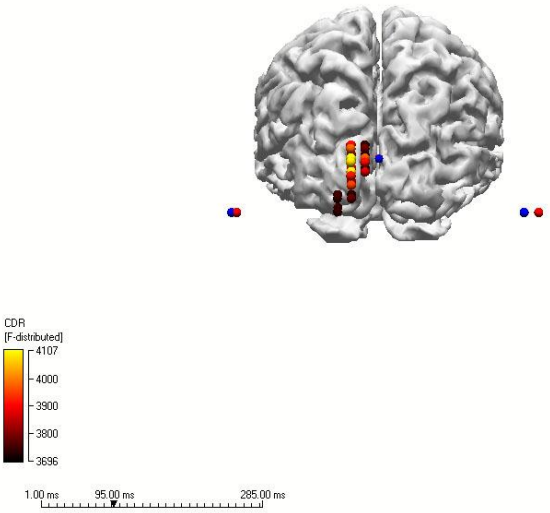

d. Right Lower

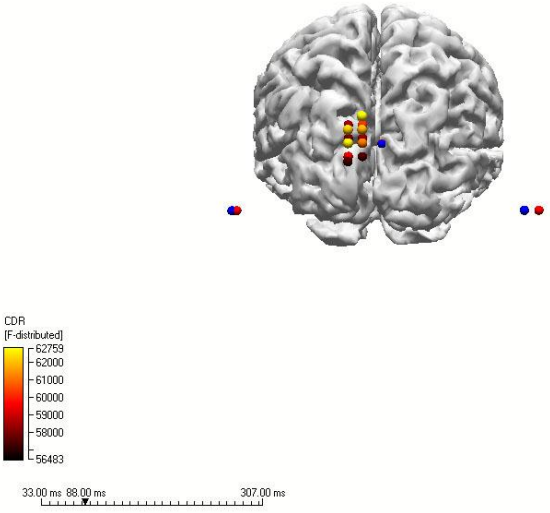

FIGURE 6. Simultaneous Recordings sLORETA F Values
a. Left Upper

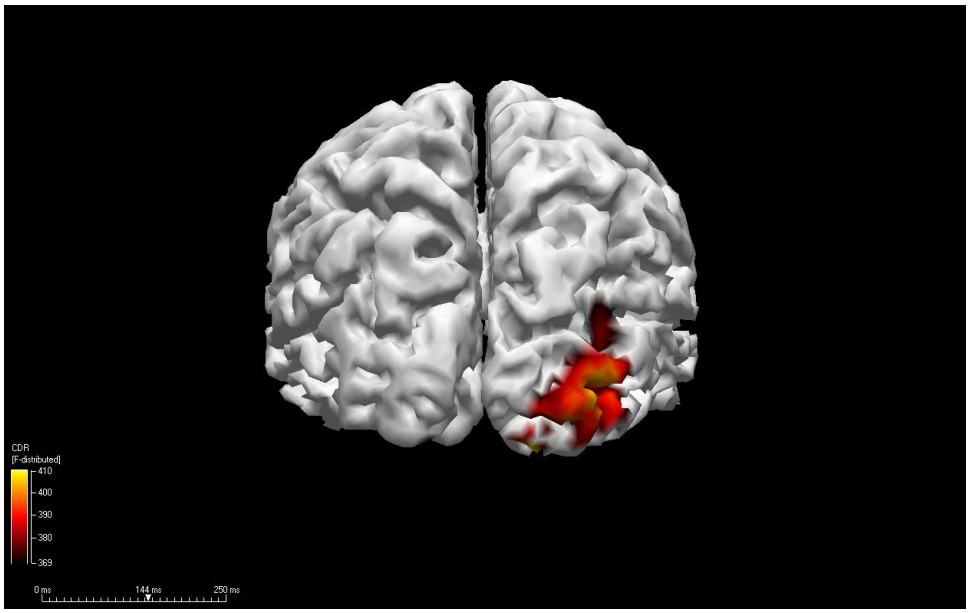

b. Left Lower

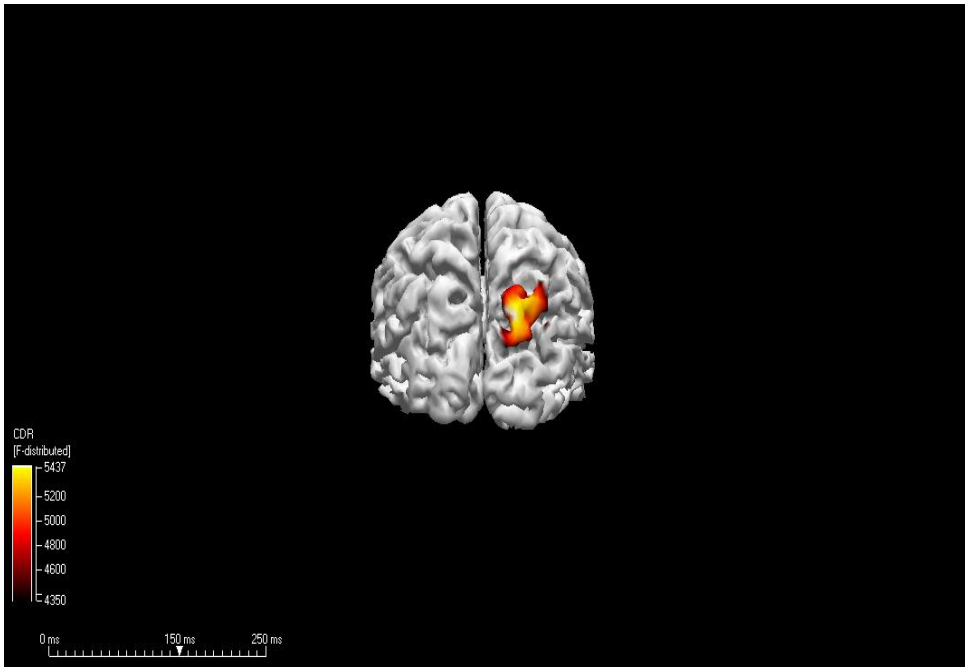

c. Right Upper

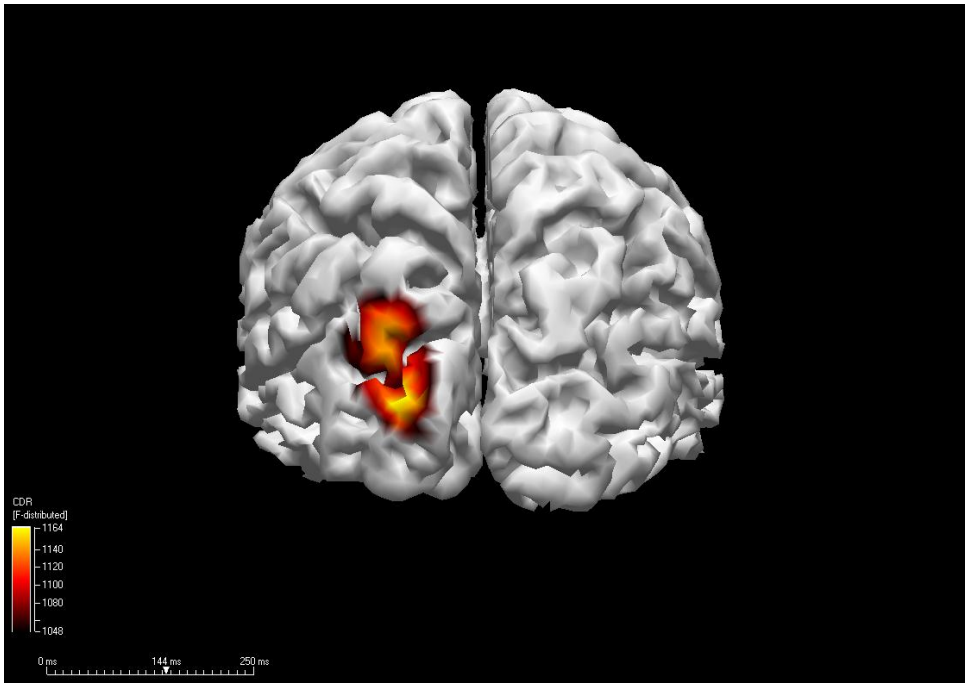

d. Right Lower

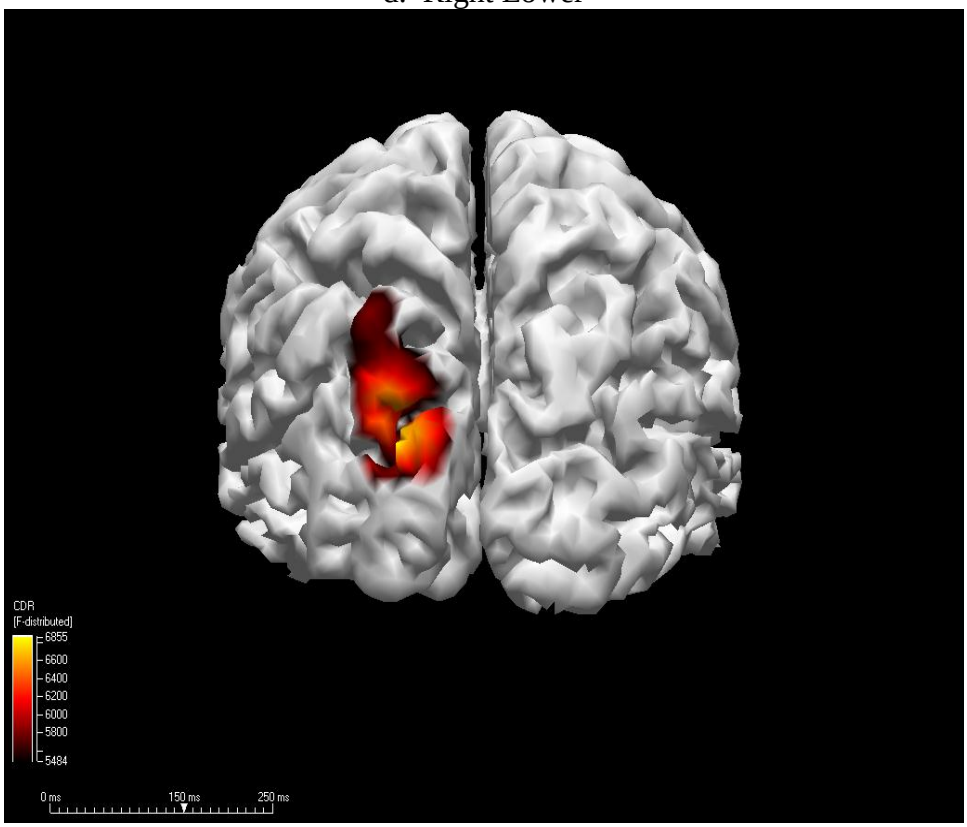

FIGURE 7. SPSS Report

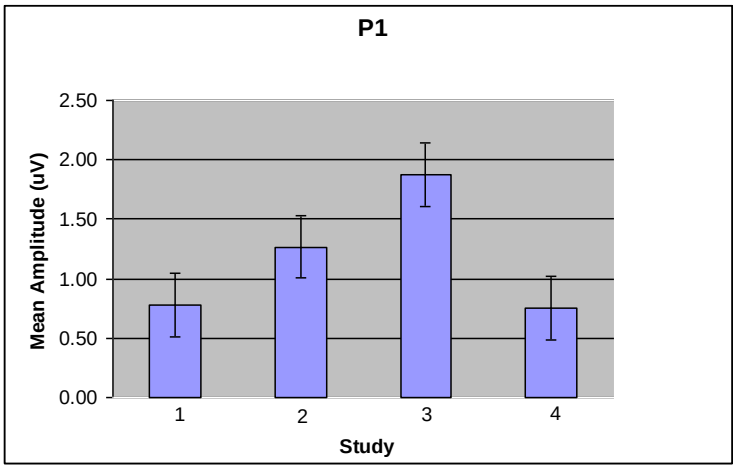


```
ONEWAY Amplitude BY Study
  /POLYNOMIAL=1
  /STATISTICS DESCRIPTIVES HOMOGENEITY
  /MISSING ANALYSIS
  /POSTHOC=TUKEY ALPHA(0.05).
```

Oneway

Warnings

Test of homogeneity of variances cannot be performed for Amplitude because only one group has a computed variance.
Post hoc tests are not performed for Amplitude because at least one group has fewer than two cases.

Descriptives

Amplitude

	N	Mean	Std. Deviation	Std. Error	95% Confidence Interval for Mean	
					Lower Bound	Upper Bound
1	1	.781459	.	.	.	.
2	1	1.267693	.	.	.	.
3	1	1.874191	.	.	.	.
4	1	.750212	.	.	.	.
Total	4	1.168389	.5268158	.2634079	.330107	2.006670

FIGURE 8. SPSS Report

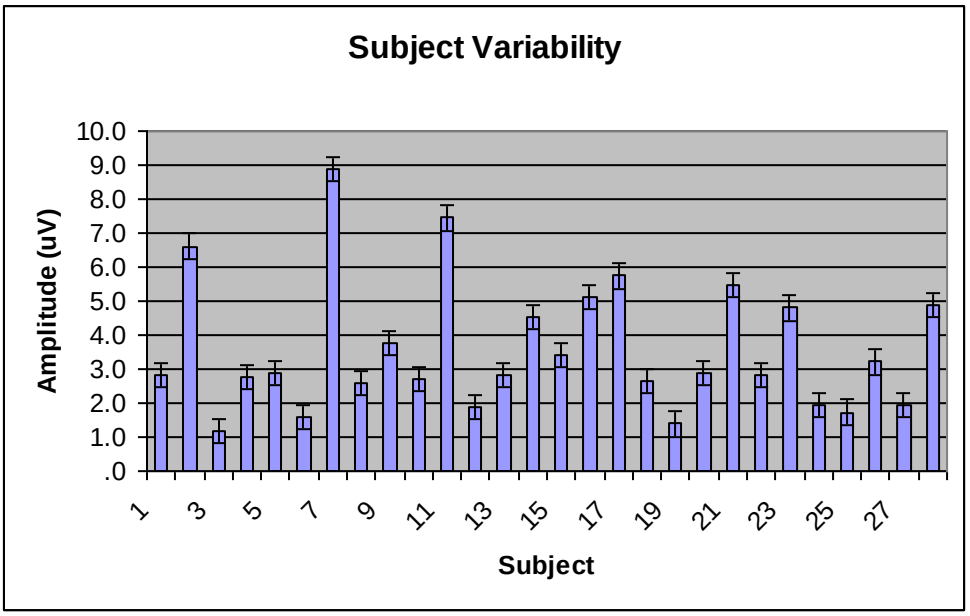

Test of homogeneity of variances cannot be performed for Amplitude because only one group has a computed variance.
Post hoc tests are not performed for Amplitude because at least one group has fewer than two cases.

Descriptives

Amplitude

	N	Mean	Std. Deviation	Std. Error	95% Confidence Interval for Mean	
					Lower Bound	Upper Bound
1	1	2.816355	.	.	.	.
2	1	6.611203	.	.	.	.
3	1	1.189103	.	.	.	.
4	1	2.758489	.	.	.	.
5	1	2.864693	.	.	.	.
6	1	1.589025	.	.	.	.
7	1	8.882474	.	.	.	.
8	1	2.591099	.	.	.	.
9	1	3.762717	.	.	.	.
10	1	2.691303	.	.	.	.
11	1	7.443878	.	.	.	.
12	1	1.867914	.	.	.	.
13	1	2.826671	.	.	.	.
14	1	4.517659	.	.	.	.
15	1	3.430772	.	.	.	.
16	1	5.109397	.	.	.	.
17	1	5.739613	.	.	.	.
18	1	2.661377	.	.	.	.
19	1	1.387667	.	.	.	.
20	1	2.865277	.	.	.	.
21	1	5.478724	.	.	.	.
22	1	2.825946	.	.	.	.
23	1	4.798571	.	.	.	.
24	1	1.930699	.	.	.	.
25	1	1.731224	.	.	.	.
26	1	3.208266	.	.	.	.
27	1	1.938713	.	.	.	.
28	1	4.876672	.	.	.	.
Total	28	3.585554	1.9183200	.3625284	2.841707	4.329400

FIGURE 9. INTRASUBJECT VARIABILIT INTERSUBJECT VARIABILITY SPSS REPORT

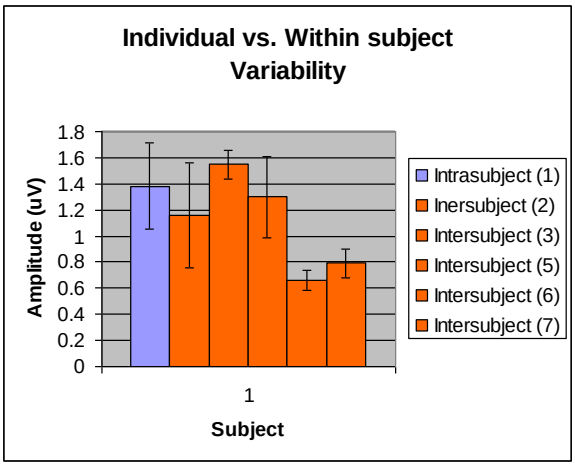


```
DATASET CLOSE DataSet3.
GET
  FILE='C:\Documents and Settings\kappametrics\My
Documents\SPSSInc\PASWStatistics18\July 26\Q1C100ST2SUB.sav'.
DATASET NAME DataSet4 WINDOW=FRONT.
ONEWAY Amplitude BY Subject
  /STATISTICS DESCRIPTIVES
  /MISSING ANALYSIS
  /POSTHOC=TUKEY ALPHA(0.05).
```

Oneway

Notes

Output Created		10-Sep-2010 14:31:30
Comments		
Input	Data	C:\Documents and Settings\kappametrics\My Documents\SPSSInc\PASWStatistics18\July 26\Q1C100ST2SUB.sav
	Active Dataset	DataSet4
	Filter	<none>
	Weight	<none>
	Split File	<none>
	N of Rows in Working Data File	18
Missing Value Handling	Definition of Missing	User-defined missing values are treated as missing.
	Cases Used	Statistics for each analysis are based on cases with no missing data for any variable in the analysis.
	Syntax	ONEWAY Amplitude BY Subject /STATISTICS DESCRIPTIVES /MISSING ANALYSIS /POSTHOC=TUKEY ALPHA(0.05).
Resources	Processor Time	00:00:00.032
	Elapsed Time	00:00:00.031

0

[DataSet4] C:\Documents and Settings\kappametrics\My Documents\SPSSInc\PASWStatistics18\July 26\Q1C100ST2SUB.sav

Descriptives

Amplitude

	N	Mean	Std. Deviation	Std. Error	95% Confidence Interval for Mean	
					Lower Bound	Upper Bound
1	3	1.381828	.5832532	.3367414	-.067053	2.830709
2	3	1.161264	.6989753	.4035536	-.575087	2.897615
3	3	1.556555	.1996104	.1152451	1.060695	2.052415
5	3	1.307781	.5474679	.3160807	-.052205	2.667767
6	3	.665595	.1465613	.0846172	.301516	1.029673
7	3	.789967	.1928641	.1113502	.310866	1.269068
Total	18	1.143832	.5016606	.1182425	.894362	1.393302

Descriptives

Amplitude

	Minimum	Maximum
1	.7815	1.9463
2	.6064	1.9463
3	1.4177	1.7853
5	.7815	1.8742
6	.5279	.8196
7	.6331	1.0053
Total	.5279	1.9463

ANOVA

Individual vs. Within subject Amplitude variability One-Way ANOVA

	Sum of Squares	df	Mean Square	F	Sig.
Between Groups	1.824	5	.365	1.784	.191
Within Groups	2.454	12	.204		
Total	4.278	17			

Post Hoc Tests

Multiple Comparisons

Amplitude Tukey HSD

(I) Subject		(J) Subject	Mean Difference (I-J)	Std. Error	Sig.	95% Confidence Interval	
						Lower Bound	Upper Bound
dimension 2	1	dimension3 2	.2205637	.3692324	.989	-1.019659	1.460786
		3	-.1747270	.3692324	.996	-1.414949	1.065495
		5	.0740470	.3692324	1.000	-1.166175	1.314269
		6	.7162333	.3692324	.426	-.523989	1.956456
		7	.5918613	.3692324	.612	-.648361	1.832084
	2	1	-.2205637	.3692324	.989	-1.460786	1.019659
		3	-.3952907	.3692324	.884	-1.635513	.844932
		5	-.1465167	.3692324	.998	-1.386739	1.093706
		6	.4956697	.3692324	.758	-.744553	1.735892
		7	.3712977	.3692324	.907	-.868925	1.611520
	3	1	.1747270	.3692324	.996	-1.065495	1.414949
		2	.3952907	.3692324	.884	-.844932	1.635513
		5	.2487740	.3692324	.982	-.991448	1.488996
		6	.8909603	.3692324	.226	-.349262	2.131183
		7	.7665883	.3692324	.359	-.473634	2.006811
	5	1	-.0740470	.3692324	1.000	-1.314269	1.166175
		2	.1465167	.3692324	.998	-1.093706	1.386739
		3	-.2487740	.3692324	.982	-1.488996	.991448
		6	.6421863	.3692324	.534	-.598036	1.882409
		7	.5178143	.3692324	.725	-.722408	1.758037
	6	1	-.7162333	.3692324	.426	-1.956456	.523989
		2	-.4956697	.3692324	.758	-1.735892	.744553
		3	-.8909603	.3692324	.226	-2.131183	.349262
		5	-.6421863	.3692324	.534	-1.882409	.598036
		7	-.1243720	.3692324	.999	-1.364594	1.115850
	7	1	-.5918613	.3692324	.612	-1.832084	.648361
		2	-.3712977	.3692324	.907	-1.611520	.868925
		3	-.7665883	.3692324	.359	-2.006811	.473634
		5	-.5178143	.3692324	.725	-1.758037	.722408
		6	.1243720	.3692324	.999	-1.115850	1.364594

Homogeneous Subsets

Amplitude

Tukey HSD[a]

Subject		N	Subset for alpha = 0.05
			1
dimension1	6	3	.665595
	7	3	.789967
	2	3	1.161264
	5	3	1.307781
	1	3	1.381828
	3	3	1.556555
	Sig.		.226

Means for groups in homogeneous subsets are displayed.

a. Uses Harmonic Mean Sample Size = 3.000.

FIGURE 10. SPSS Report

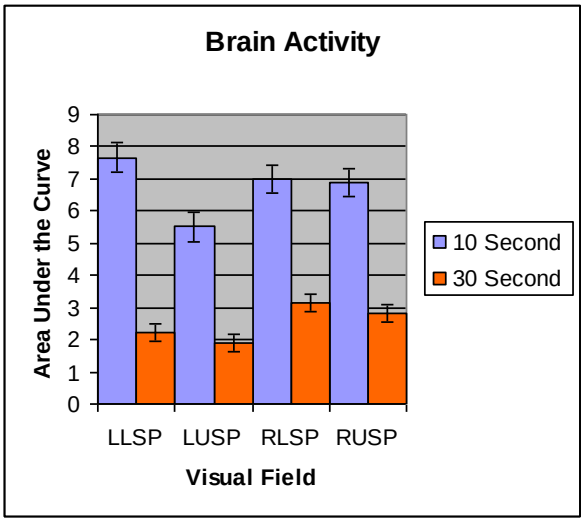

Descriptives amplidute

	N	Mean	Std. Deviation	Std. Error	95% Confidence Interval for Mean	
					Lower Bound	Upper Bound
30 sec	4	2.5150	.56977	.28488	1.6084	3.4216
10 sec	4	6.7625	.90373	.45187	5.3244	8.2005
Total	8	4.6387	2.37566	.83992	2.6526	6.6248

Descriptives

amplidute

	Minimum	Maximum
30 sec	1.88	3.14
10 sec	5.51	7.66
Total	1.88	7.66

ANOVA

amplidute

	Sum of Squares	df	Mean Square	F	Sig.
Between Groups	36.082	1	36.082	63.226	.000
Within Groups	3.424	6	.571		
Total	39.506	7			

FIGURE 11 EXPERIMENT 2 P1, N1, AND P2 AMPLITUDE VARIABLITY

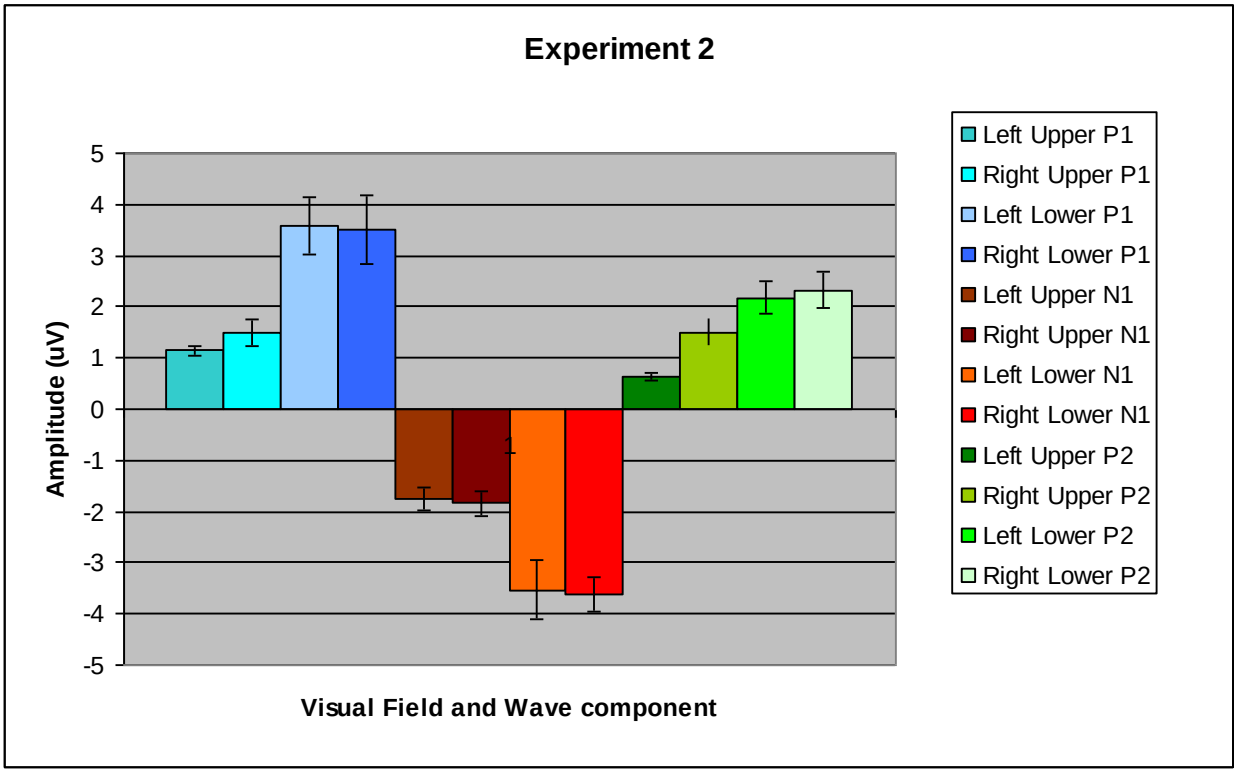


```
Q1234C1EXP2
GET
  FILE='C:\Documents and Settings\kappametrics\My
Documents\SPSSInc\PASWStatistics18\July 26\September\Q1234C100Exp2.sav'.
DATASET NAME DataSet17 WINDOW=FRONT.
ONEWAY Amplitude BY Electrode
  /POLYNOMIAL=1
  /STATISTICS DESCRIPTIVES EFFECTS HOMOGENEITY
  /MISSING ANALYSIS
  /POSTHOC=TUKEY ALPHA(0.05).
```

P1 Oneway

Notes

Output Created		10-Sep-2010 17:27:48
Comments		
Input	Data	C:\Documents and Settings\kappametrics\My Documents\SPSSInc\PASWStatistics18\July 26\September\Q1234C100Exp2.sav
	Active Dataset	DataSet17
	Filter	<none>
	Weight	<none>
	Split File	<none>

	N of Rows in Working Data File	68
Missing Value Handling	Definition of Missing	User-defined missing values are treated as missing.
	Cases Used	Statistics for each analysis are based on cases with no missing data for any variable in the analysis.
Syntax		ONEWAY Amplitude BY Electrode /POLYNOMIAL=1 /STATISTICS DESCRIPTIVES EFFECTS HOMOGENEITY /MISSING ANALYSIS /POSTHOC=TUKEY ALPHA(0.05).
Resources	Processor Time	00:00:00.032
	Elapsed Time	00:00:00.031

[DataSet17] C:\Documents and Settings\kappametrics\My Documents\SPSSInc\PASWStatistics18\July 26\September\Q1234C100Exp2.sav

Descriptives

Amplitude

		N	Mean	Std. Deviation	Std. Error
58 PO7 RU		16	1.508288	1.0684428	.2671107
59 PO3 RL		18	3.526518	2.8635917	.6749550
61 PO4 LL		15	3.228975	2.0639121	.5328998
62 PO8 LU		19	1.141014	.4879397	.1119410
Total		68	2.319468	2.1018687	.2548890
Model	Fixed Effects			1.8559365	.2250654
	Random Effects				.6115811

Descriptives

Amplitude

		95% Confidence Interval for Mean		Minimum	Maximum	Between-Component Variance
		Lower Bound	Upper Bound			
58 PO7 RU		.938955	2.077621	.0738	3.5897	
59 PO3 RL		2.102488	4.950549	.2809	9.5420	
61 PO4 LL		2.086019	4.371932	.3637	8.2409	
62 PO8 LU		.905835	1.376193	.5279	1.9463	
Total		1.810708	2.828229	.0738	9.5420	
Model	Fixed Effects	1.869848	2.769088			
	Random Effects	.373144	4.265792			1.2824146

Test of Homogeneity of Variances

Amplitude

Levene Statistic	df1	df2	Sig.
13.481	3	64	.000

ANOVA

Amplitude

			Sum of Squares	df	Mean Square
Between Groups	(Combined)		75.548	3	25.183
	Linear Term	Weighted	4.188	1	4.188
		Deviation	71.360	2	35.680
Within Groups			220.448	64	3.445
Total			295.996	67	

ANOVA

Amplitude

			F	Sig.
Between Groups	(Combined)		7.311	.000
	Linear Term	Weighted	1.216	.274
		Deviation	10.358	.000

Post Hoc Tests

Multiple Comparisons

Amplitude Tukey HSD

(I) Electrode	(J) Electrode	Mean Difference (I-J)	Std. Error	Sig.	95% Confidence Interval	
					Lower Bound	Upper Bound
58	59	-2.0182306*	.6376852	.012	-3.700341	-.336120
	61	-1.7206873	.6670192	.058	-3.480176	.038802
	62	.3672738	.6297386	.937	-1.293875	2.028423
59	58	2.0182306*	.6376852	.012	.336120	3.700341
	61	.2975433	.6488409	.968	-1.413994	2.009081
	62	2.3855044*	.6104512	.001	.775233	3.995776
61	58	1.7206873	.6670192	.058	-.038802	3.480176
	59	-.2975433	.6488409	.968	-2.009081	1.413994
	62	2.0879611*	.6410326	.010	.397020	3.778902
62	58	-.3672738	.6297386	.937	-2.028423	1.293875
	59	-2.3855044*	.6104512	.001	-3.995776	-.775233
	61	-2.0879611*	.6410326	.010	-3.778902	-.397020

*. The mean difference is significant at the 0.05 level.

Homogeneous Subsets

Amplitude

Tukey HSD[a,b]

Electrode	N	Subset for alpha = 0.05	
		1	2
62	19	1.141014	
58	16	1.508288	
61	15		3.228975
59	18		3.526518
Sig.		.939	.966

Means for groups in homogeneous subsets are displayed.

a. Uses Harmonic Mean Sample Size = 16.852.

Amplitude

Tukey HSD[a,b]

Electrode	N	Subset for alpha = 0.05	
		1	2
62	19	1.141014	
58	16	1.508288	
61	15		3.228975
59	18		3.526518
Sig.		.939	.966

Means for groups in homogeneous subsets are displayed.

a. Uses Harmonic Mean Sample Size = 16.852.

b. The group sizes are unequal. The harmonic mean of the group sizes is used. Type I error levels are not guaranteed.

Q1234C2EXP2

```
GET
  FILE='C:\Documents and Settings\kappametrics\My
Documents\SPSSInc\PASWStatistics18\July 26\September\Q1234C200Exp2.sav'.
DATASET NAME DataSet18 WINDOW=FRONT.
ONEWAY Amplitude BY Electrode
  /POLYNOMIAL=1
  /STATISTICS DESCRIPTIVES EFFECTS HOMOGENEITY
  /MISSING ANALYSIS
  /POSTHOC=TUKEY ALPHA(0.05).
```

N1 One-way ANOVA

Notes

Output Created		10-Sep-2010 17:30:08
Comments		
Input	Data	C:\Documents and Settings\kappametrics\My Documents\SPSSInc\PASWStatistics18\July 26\September\Q1234C200Exp2.sav
	Active Dataset	DataSet18
	Filter	<none>
	Weight	<none>
	Split File	<none>
	N of Rows in Working Data File	70
Missing Value Handling	Definition of Missing	User-defined missing values are treated as missing.
	Cases Used	Statistics for each analysis are based on cases with no missing data for any variable in the analysis.
Syntax		ONEWAY Amplitude BY Electrode /POLYNOMIAL=1 /STATISTICS DESCRIPTIVES EFFECTS HOMOGENEITY /MISSING ANALYSIS /POSTHOC=TUKEY ALPHA(0.05).
Resources	Processor Time	00:00:00.016
	Elapsed Time	00:00:00.031

[DataSet18] C:\Documents and Settings\kappametrics\My Documents\SPSSInc\PASWStatistics18\July 26\September\Q1234C200Exp2.sav

Descriptives

Amplitude

		N	Mean	Std. Deviation	Std. Error
58 PO7 RU		15	-1.840137	1.1963786	.3089036
59 PO3 RL		18	-3.633982	1.4399335	.3393956
61 PO4 LL		19	-3.531924	2.5596137	.5872156
62 PO8 LU		18	-1.748566	1.0041100	.2366710
Total		70	-2.737064	1.8900799	.2259078
Model	Fixed Effects			1.6982864	.2029841
	Random Effects				.5191862

Descriptives

Amplitude

		95% Confidence Interval for Mean		Minimum	Maximum	Between-Component Variance
		Lower Bound	Upper Bound			
58 PO7 RU		-2.502669	-1.177604	-4.7540	-.2495	
59 PO3 RL		-4.350044	-2.917920	-6.3873	-.9665	
61 PO4 LL		-4.765618	-2.298230	-11.2457	-.2020	
62 PO8 LU		-2.247898	-1.249234	-3.9782	-.2592	
Total		-3.187737	-2.286390	-11.2457	-.2020	
Model	Fixed Effects	-3.142335	-2.331793			
	Random Effects	-4.389346	-1.084782			.9067452

Test of Homogeneity of Variances

Amplitude

Levene Statistic	df1	df2	Sig.
4.440	3	66	.007

ANOVA

Amplitude

			Sum of Squares	df	Mean Square
Between Groups	(Combined)		56.140	3	18.713
	Linear Term	Weighted	.561	1	.561
		Deviation	55.579	2	27.789
Within Groups			190.356	66	2.884
Total			246.496	69	

ANOVA

Amplitude

			F	Sig.
Between Groups	(Combined)		6.488	.001
	Linear Term	Weighted	.195	.661
		Deviation	9.635	.000

Post Hoc Tests

Multiple Comparisons

Amplitude
Tukey HSD

(I) Electrode	(J) Electrode	Mean Difference (I-J)	Std. Error	Sig.	95% Confidence Interval	
					Lower Bound	Upper Bound
58	59	1.7938456*	.5937259	.018	.228954	3.358738
	61	1.6917874*	.5865810	.027	.145728	3.237847
	62	-.0915710	.5937259	.999	-1.656463	1.473321
59	58	-1.7938456*	.5937259	.018	-3.358738	-.228954
	61	-.1020582	.5585972	.998	-1.574361	1.370244
	62	-1.8854166*	.5660955	.008	-3.377482	-.393351
61	58	-1.6917874*	.5865810	.027	-3.237847	-.145728
	59	.1020582	.5585972	.998	-1.370244	1.574361
	62	-1.7833584*	.5585972	.011	-3.255661	-.311056
62	58	.0915710	.5937259	.999	-1.473321	1.656463
	59	1.8854166*	.5660955	.008	.393351	3.377482
	61	1.7833584*	.5585972	.011	.311056	3.255661

*. The mean difference is significant at the 0.05 level.

Homogeneous Subsets

Amplitude

Tukey HSD[a,b]

Electrode	N	Subset for alpha = 0.05	
		1	2
59	18	-3.633982	
61	19	-3.531924	
58	15		-1.840137
62	18		-1.748566
Sig.		.998	.999

Means for groups in homogeneous subsets are displayed.
a. Uses Harmonic Mean Sample Size = 17.360.
b. The group sizes are unequal. The harmonic mean of the group sizes is used. Type I error levels are not guaranteed.

Q1234C3EXP2

```
DATASET ACTIVATE DataSet13.
DATASET CLOSE DataSet19.
DATASET ACTIVATE DataSet17.
DATASET CLOSE DataSet13.
GET
  FILE='C:\Documents and Settings\kappametrics\My
Documents\SPSSInc\PASWStatistics18\July 26\Q1C300.sav'.
DATASET NAME DataSet20 WINDOW=FRONT.
DATASET ACTIVATE DataSet17.
GET
  FILE='C:\Documents and Settings\kappametrics\My
Documents\SPSSInc\PASWStatistics18\July 26\Q2C300.sav'.
DATASET NAME DataSet21 WINDOW=FRONT.
DATASET ACTIVATE DataSet17.
DATASET CLOSE DataSet21.
GET
  FILE='C:\Documents and Settings\kappametrics\My
Documents\SPSSInc\PASWStatistics18\July 26\Q3C300.sav'.
DATASET NAME DataSet22 WINDOW=FRONT.
DATASET ACTIVATE DataSet17.
GET
  FILE='C:\Documents and Settings\kappametrics\My
Documents\SPSSInc\PASWStatistics18\July 26\Q4C300.sav'.
DATASET NAME DataSet23 WINDOW=FRONT.
DATASET ACTIVATE DataSet18.
DATASET CLOSE DataSet17.
DATASET ACTIVATE DataSet20.
DATASET CLOSE DataSet18.

SAVE OUTFILE='C:\Documents and Settings\kappametrics\My
Documents\SPSSInc\PASWStatistics18\July '+
    '26\September\Q1234C300Exp2.sav'
  /COMPRESSED.
ONEWAY Amplitude BY Electrode
  /POLYNOMIAL=1
  /STATISTICS DESCRIPTIVES EFFECTS HOMOGENEITY
  /PLOT MEANS
  /MISSING ANALYSIS
  /POSTHOC=TUKEY ALPHA(0.05).
```

P2 Oneway

Notes

Output Created		10-Sep-2010 17:36:44
Comments		
Input	Data	C:\Documents and Settings\kappametrics\My Documents\SPSSInc\PASWStatistics18\July 26\September\Q1234C300Exp2.sav
	Active Dataset	DataSet20
	Filter	<none>
	Weight	<none>
	Split File	<none>
	N of Rows in Working Data File	65
Missing Value Handling	Definition of Missing	User-defined missing values are treated as missing.
	Cases Used	Statistics for each analysis are based on cases with no missing data for any variable in the analysis.
Syntax		ONEWAY Amplitude BY Electrode /POLYNOMIAL=1 /STATISTICS DESCRIPTIVES EFFECTS HOMOGENEITY /PLOT MEANS /MISSING ANALYSIS /POSTHOC=TUKEY ALPHA(0.05).
Resources	Processor Time	00:00:00.468
	Elapsed Time	00:00:00.452

[DataSet20] C:\Documents and Settings\kappametrics\My Documents\SPSSInc\PASWStatistics18\July 26\September\Q1234C300Exp2.sav

Descriptives

Amplitude

		N	Mean	Std. Deviation	Std. Error
58 PO7 RU		11	1.5073648	.93152540	.28086548
59 PO3 RL		18	1.7624352	1.79650071	.42343928
61 PO4 LL		19	2.1801258	1.40564961	.32247814
62 PO8 LU		17	.6307862	.35625530	.08640460
Total		65	1.5453939	1.39126018	.17256459
Model	Fixed Effects			1.28764270	.15971242
	Random Effects				.34802749

Descriptives

Amplitude

		95% Confidence Interval for Mean		Minimum	Maximum	Between-Component Variance
		Lower Bound	Upper Bound			
58 PO7 RU		.8815575	2.1331721	.12946	2.66913	
59 PO3 RL		.8690564	2.6558140	-1.39461	4.46920	
61 PO4 LL		1.5026244	2.8576273	.07081	5.49124	
62 PO8 LU		.4476166	.8139557	.21578	1.26027	
Total		1.2006565	1.8901313	-1.39461	5.49124	
Model	Fixed Effects	1.2260292	1.8647586			
	Random Effects	.4378151	2.6529727			.36892575

Test of Homogeneity of Variances

Amplitude

Levene Statistic	df1	df2	Sig.
7.262	3	61	.000

ANOVA

Amplitude

			Sum of Squares	df	Mean Square
Between Groups	(Combined)		22.739	3	7.580
	Linear Term	Weighted	3.338	1	3.338
		Deviation	19.401	2	9.701
Within Groups			101.139	61	1.658
Total			123.879	64	

ANOVA

Amplitude

			F	Sig.
Between Groups	(Combined)		4.572	.006
	Linear Term	Weighted	2.013	.161
		Deviation	5.851	.005

Post Hoc Tests

Multiple Comparisons

Amplitude Tukey HSD

(I) Electrode	(J) Electrode	Mean Difference (I-J)	Std. Error	Sig.	95% Confidence Interval	
					Lower Bound	Upper Bound
58	59	-.25507040	.49278987	.955	-1.5566722	1.0465314
	61	-.67276102	.48784612	.517	-1.9613050	.6157829
	62	.87657864	.49825720	.303	-.4394640	2.1926213
59	58	.25507040	.49278987	.955	-1.0465314	1.5566722
	61	-.41769062	.42352903	.758	-1.5363544	.7009731
	62	1.13164905	.43548047	.055	-.0185819	2.2818800
61	58	.67276102	.48784612	.517	-.6157829	1.9613050
	59	.41769062	.42352903	.758	-.7009731	1.5363544
	62	1.54933967*	.42987814	.003	.4139061	2.6847733
62	58	-.87657864	.49825720	.303	-2.1926213	.4394640
	59	-1.13164905	.43548047	.055	-2.2818800	.0185819
	61	-1.54933967*	.42987814	.003	-2.6847733	-.4139061

*. The mean difference is significant at the 0.05 level.

Homogeneous Subsets

Amplitude

Tukey HSD[a,b]

Electrode	N	Subset for alpha = 0.05	
		1	2
62	17	.6307862	
58	11	1.5073648	1.5073648
59	18	1.7624352	1.7624352
61	19		2.1801258
Sig.		.079	.471

Means for groups in homogeneous subsets are displayed.

a. Uses Harmonic Mean Sample Size = 15.509.

b. The group sizes are unequal. The harmonic mean of the group sizes is used. Type I error levels are not guaranteed.

FIGURE 12 EXPERIMENT 3 P1, N1, AND P2 AMPLITUDE VARIABLITY

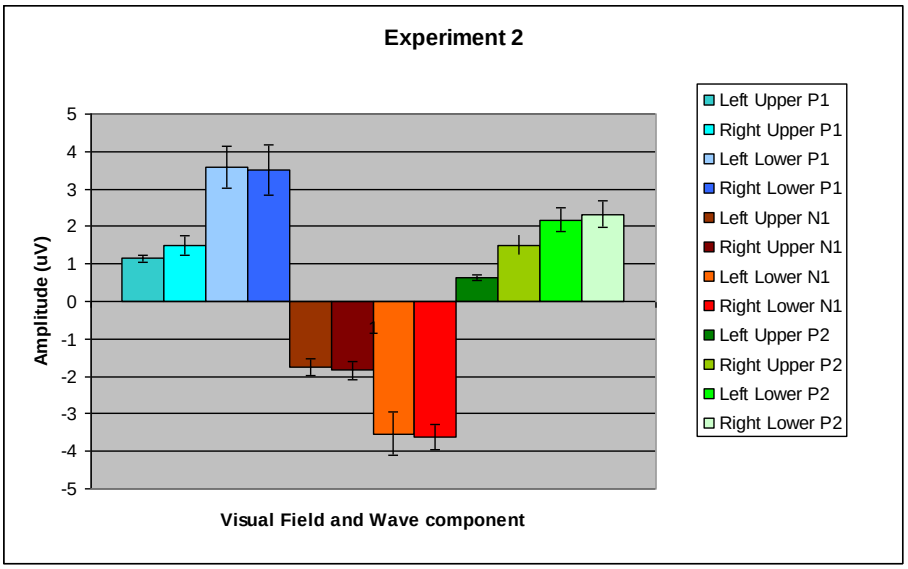


```
GET
  FILE='C:\Documents and Settings\kappametrics\My
Documents\SPSSInc\PASWStatistics18\July 26\Q1234C100.sav'.
DATASET NAME DataSet1 WINDOW=FRONT.
ONEWAY Amplitude BY Electrode
  /POLYNOMIAL=1
  /STATISTICS DESCRIPTIVES EFFECTS HOMOGENEITY
  /PLOT MEANS
  /MISSING ANALYSIS
  /POSTHOC=TUKEY ALPHA(0.05).
```

P1 Oneway

Notes

Output Created		10-Sep-2010 16:00:20
Comments		
Input	Data	C:\Documents and Settings\kappametrics\My Documents\SPSSInc\PASWStatistics18\July 26\Q1234C100.sav
	Active Dataset	DataSet1
	Filter	<none>
	Weight	<none>
	Split File	<none>
	N of Rows in Working Data File	108
Missing Value Handling	Definition of Missing	User-defined missing values are treated as missing.
	Cases Used	Statistics for each analysis are based on cases with no missing data for any variable in the analysis.
Syntax		ONEWAY Amplitude BY Electrode /POLYNOMIAL=1 /STATISTICS DESCRIPTIVES EFFECTS HOMOGENEITY /PLOT MEANS /MISSING ANALYSIS /POSTHOC=TUKEY ALPHA(0.05).
Resources	Processor Time	00:00:00.563
	Elapsed Time	00:00:00.890

[DataSet1] C:\Documents and Settings\kappametrics\My Documents\SPSSInc\PASWStatistics18\July 26\Q1234C100.sav

Descriptives

Amplitude

	N	Mean	Std. Deviation	Std. Error
58	26	3.835231	1.9194369	.3764325
59	25	4.469571	2.3933993	.4786799
61	29	3.796057	2.2384182	.4156638
62	28	3.585554	1.9183200	.3625284

	Total	108	3.906819	2.1191956	.2039197
Model	Fixed Effects			2.1241282	.2043943
	Random Effects				.2043943[a]

a. Warning: Between-component variance is negative. It was replaced by 0.0 in computing this random effects measure.

Descriptives

Amplitude

		95% Confidence Interval for Mean				
		Lower Bound	Upper Bound	Minimum	Maximum	Between-Component Variance
	58	3.059954	4.610509	.7591	8.5901	
	59	3.481625	5.457518	1.6701	12.0088	
	61	2.944608	4.647506	.9325	10.2834	
	62	2.841707	4.329400	1.1891	8.8825	
	Total	3.502572	4.311066	.7591	12.0088	
Model	Fixed Effects	3.501497	4.312141			
	Random Effects	3.256345[a]	4.557293[a]			-.0276806

a. Warning: Between-component variance is negative. It was replaced by 0.0 in computing this random effects measure.

Test of Homogeneity of Variances

Amplitude

Levene Statistic	df1	df2	Sig.
.106	3	104	.956

ANOVA

Amplitude

			Sum of Squares	df	Mean Square
Between Groups	(Combined)		11.296	3	3.765
	Linear Term	Weighted	3.695	1	3.695
		Deviation	7.602	2	3.801
Within Groups			469.240	104	4.512
Total			480.536	107	

ANOVA

Amplitude

			F	Sig.
Between Groups	(Combined)		.835	.478
	Linear Term	Weighted	.819	.368
		Deviation	.842	.434

Post Hoc Tests

Multiple Comparisons

Amplitude

Tukey HSD

(I) Electrode	(J) Electrode	Mean Difference (I-J)	Std. Error	Sig.	95% Confidence Interval	
					Lower Bound	Upper Bound
58	59	-.6343399	.5949893	.711	-2.187892	.919212
	61	.0391744	.5736888	1.000	-1.458761	1.537110
	62	.2496777	.5785114	.973	-1.260850	1.760205
59	58	.6343399	.5949893	.711	-.919212	2.187892
	61	.6735144	.5797071	.652	-.840135	2.187164
	62	.8840177	.5844800	.434	-.642094	2.410129
61	58	-.0391744	.5736888	1.000	-1.537110	1.458761
	59	-.6735144	.5797071	.652	-2.187164	.840135
	62	.2105033	.5627819	.982	-1.258954	1.679960
62	58	-.2496777	.5785114	.973	-1.760205	1.260850
	59	-.8840177	.5844800	.434	-2.410129	.642094
	61	-.2105033	.5627819	.982	-1.679960	1.258954

Homogeneous Subsets

Amplitude

Tukey HSD[a,b]

Electrode	N	Subset for alpha = 0.05
		1
62	28	3.585554
61	29	3.796057
58	26	3.835231
59	25	4.469571
Sig.		.425

Means for groups in homogeneous subsets are displayed.

a. Uses Harmonic Mean Sample Size = 26.907.

b. The group sizes are unequal. The harmonic mean of the group sizes is used. Type I error levels are not guaranteed.

N1 Oneway

```
GET
FILE='C:\Documents and Settings\kappametrics\My Documents\SPSSInc\PASWStatistics18\July 26\Q1234C200.sav'.
DATASET NAME DataSet2 WINDOW=FRONT.
ONEWAY Amplitude BY Electrode
/POLYNOMIAL=1
/STATISTICS DESCRIPTIVES EFFECTS HOMOGENEITY
/MISSING ANALYSIS
/POSTHOC=TUKEY ALPHA(0.05).
```

Notes

Output Created		10-Sep-2010 16:05:39
Comments		
Input	Data	C:\Documents and Settings\kappametrics\My Documents\SPSSInc\PASWStatistics18\July 26\Q1234C200.sav
	Active Dataset	DataSet2
	Filter	<none>
	Weight	<none>
	Split File	<none>
	N of Rows in Working Data File	105
Missing Value Handling	Definition of Missing	User-defined missing values are treated as missing.
	Cases Used	Statistics for each analysis are based on cases with no missing data for any variable in the analysis.
Syntax		ONEWAY Amplitude BY Electrode /POLYNOMIAL=1 /STATISTICS DESCRIPTIVES EFFECTS HOMOGENEITY /MISSING ANALYSIS /POSTHOC=TUKEY ALPHA(0.05).
Resources	Processor Time	00:00:00.031
	Elapsed Time	00:00:00.031

[DataSet2] C:\Documents and Settings\kappametrics\My Documents\SPSSInc\PASWStatistics18\July 26\Q1234C200.sav

Descriptives

Amplitude

		N	Mean	Std. Deviation	Std. Error
58 PO7 RU		23	-1.253710	.8006440	.1669458
59 PO3 RL		28	-4.599171	2.3427238	.4427332
61 PO4 LL		30	-5.594968	2.8650731	.5230884
62 PO8 LU		24	-1.752931	1.2493661	.2550258
Total		105	-3.500300	2.7579317	.2691466
Model	Fixed Effects			2.0782704	.2028184

Descriptives

Amplitude

		N	Mean	Std. Deviation	Std. Error
58 PO7 RU		23	-1.253710	.8006440	.1669458
59 PO3 RL		28	-4.599171	2.3427238	.4427332
61 PO4 LL		30	-5.594968	2.8650731	.5230884
62 PO8 LU		24	-1.752931	1.2493661	.2550258
	Total	105	-3.500300	2.7579317	.2691466
Model	Fixed Effects			2.0782704	.2028184
	Random Effects				1.0694025

Descriptives

Amplitude

		95% Confidence Interval for Mean		Minimum	Maximum	Between-Component Variance
		Lower Bound	Upper Bound			
58 PO7 RU		-1.599934	-.907485	-2.9110	-.1772	
59 PO3 RL		-5.507585	-3.690758	-11.4904	-.4923	
61 PO4 LL		-6.664804	-4.525132	-12.2953	-.4108	
62 PO8 LU		-2.280492	-1.225370	-4.1441	-.1334	
	Total	-4.034028	-2.966572	-12.2953	-.1334	
Model	Fixed Effects	-3.902637	-3.097963			
	Random Effects	-6.903616	-.096984			4.3581615

Test of Homogeneity of Variances

Amplitude

Levene Statistic	df1	df2	Sig.
9.076	3	101	.000

ANOVA

Amplitude

			Sum of Squares	df	Mean Square
Between Groups	(Combined)		354.804	3	118.268
	Linear Term	Weighted	10.805	1	10.805
		Deviation	343.998	2	171.999
	Within Groups		436.240	101	4.319
	Total		791.043	104	

ANOVA

Amplitude

			F	Sig.
Between Groups	(Combined)		27.382	.000
	Linear Term	Weighted	2.502	.117
		Deviation	39.822	.000

Post Hoc Tests

Multiple Comparisons

Amplitude

Tukey HSD

(I) Electrode	(J) Electrode	Mean Difference (I-J)	Std. Error	Sig.	95% Confidence Interval	
					Lower Bound	Upper Bound
58	59	3.3454615*	.5848496	.000	1.817645	4.873277
	61	4.3412582*	.5759907	.000	2.836585	5.845932
	62	.4992216	.6064311	.843	-1.084972	2.083415
59	58	-3.3454615*	.5848496	.000	-4.873277	-1.817645
	61	.9957967	.5461053	.268	-.430807	2.422400
	62	-2.8462399*	.5781215	.000	-4.356480	-1.336000
61	58	-4.3412582*	.5759907	.000	-5.845932	-2.836585
	59	-.9957967	.5461053	.268	-2.422400	.430807
	62	-3.8420366*	.5691578	.000	-5.328860	-2.355213
62	58	-.4992216	.6064311	.843	-2.083415	1.084972
	59	2.8462399*	.5781215	.000	1.336000	4.356480
	61	3.8420366*	.5691578	.000	2.355213	5.328860

*. The mean difference is significant at the 0.05 level.

Homogeneous Subsets

Amplitude

Tukey HSD[a,b]

Electrode	N	Subset for alpha = 0.05	
		1	2
61	30	-5.594968	
59	28	-4.599171	
62	24		-1.752931
58	23		-1.253710
Sig.		.316	.823

Means for groups in homogeneous subsets are displayed.

a. Uses Harmonic Mean Sample Size = 25.942.

b. The group sizes are unequal. The harmonic mean of the group sizes is used. Type I error levels are not guaranteed.

/MISSING ANALYSIS
/POSTHOC=TUKEY ALPHA(0.05).

P2 Oneway

Notes

Output Created		10-Sep-2010 16:08:08
Comments		
Input	Data	C:\Documents and Settings\kappametrics\My Documents\SPSSInc\PASWStatistics18\July 26\Q1234C300.sav
	Active Dataset	DataSet3
	Filter	<none>
	Weight	<none>
	Split File	<none>
	N of Rows in Working Data File	108
Missing Value Handling	Definition of Missing	User-defined missing values are treated as missing.
	Cases Used	Statistics for each analysis are based on cases with no missing data for any variable in the analysis.
Syntax		ONEWAY Amplitude BY Electrode /POLYNOMIAL=1 /STATISTICS DESCRIPTIVES EFFECTS HOMOGENEITY /MISSING ANALYSIS /POSTHOC=TUKEY ALPHA(0.05).
Resources	Processor Time	00:00:00.031
	Elapsed Time	00:00:00.031

[DataSet3] C:\Documents and Settings\kappametrics\My Documents\SPSSInc\PASWStatistics18\July 26\Q1234C300.sav

Descriptives

Amplitude

		N	Mean	Std. Deviation	Std. Error
58 PO7 RU		24	.871591	.5941125	.1212727
59 PO3 RL		27	1.169061	.8270625	.1591683
61 PO4 LL		30	1.681500	1.4039544	.2563258
62 PO8 LU		27	.872899	.5762045	.1108906
	Total	108	1.171260	.9861955	.0948967
Model	Fixed Effects			.9389898	.0903543
	Random Effects				.1960209

Descriptives Amplitude

		95% Confidence Interval for Mean		Minimum	Maximum	Between-Component Variance
		Lower Bound	Upper Bound			
58 PO7 RU		.620719	1.122463	.0344	1.9752	
59 PO3 RL		.841886	1.496236	.2823	4.2445	
61 PO4 LL		1.157255	2.205745	.3494	7.1780	
62 PO8 LU		.644960	1.100838	.1012	2.1940	
	Total	.983139	1.359382	.0344	7.1780	
Model	Fixed Effects	.992084	1.350436			
	Random Effects	.547435	1.795086			.1202985

Test of Homogeneity of Variances

Amplitude

Levene Statistic	df1	df2	Sig.
2.525	3	104	.062

ANOVA Amplitude

			Sum of Squares	df	Mean Square
Between Groups	(Combined)		12.369	3	4.123
	Linear Term	Weighted	.715	1	.715
		Deviation	11.654	2	5.827
Within Groups			91.697	104	.882
Total			104.066	107	

ANOVA

Amplitude

			F	Sig.
Between Groups	(Combined)		4.676	.004
	Linear Term	Weighted	.811	.370
		Deviation	6.609	.002

Post Hoc Tests

Multiple Comparisons

Amplitude

Tukey HSD

(I) Electrode	(J) Electrode	Mean Difference (I-J)	Std. Error	Sig.	95% Confidence Interval	
					Lower Bound	Upper Bound
58	59	-.2974702	.2634259	.672	-.985291	.390350
	61	-.8099090*	.2571530	.011	-1.481351	-.138467
	62	-.0013079	.2634259	1.000	-.689128	.686513
59	58	.2974702	.2634259	.672	-.390350	.985291
	61	-.5124388	.2490897	.174	-1.162827	.137949
	62	.2961623	.2555607	.654	-.371122	.963446
61	58	.8099090*	.2571530	.011	.138467	1.481351
	59	.5124388	.2490897	.174	-.137949	1.162827
	62	.8086011*	.2490897	.008	.158213	1.458989
62	58	.0013079	.2634259	1.000	-.686513	.689128
	59	-.2961623	.2555607	.654	-.963446	.371122
	61	-.8086011*	.2490897	.008	-1.458989	-.158213

*. The mean difference is significant at the 0.05 level.

Homogeneous Subsets

Amplitude

Tukey HSD[a,b]

Electrode	N	Subset for alpha = 0.05	
		1	2
58	24	.871591	
62	27	.872899	
59	27	1.169061	1.169061
61	30		1.681500
Sig.		.653	.195

Means for groups in homogeneous subsets are displayed.

a. Uses Harmonic Mean Sample Size = 26.832.

b. The group sizes are unequal. The harmonic mean of the group sizes is used. Type I error levels are not guaranteed.

FIGURE 13. sLORETA F values.

a. Left Upper

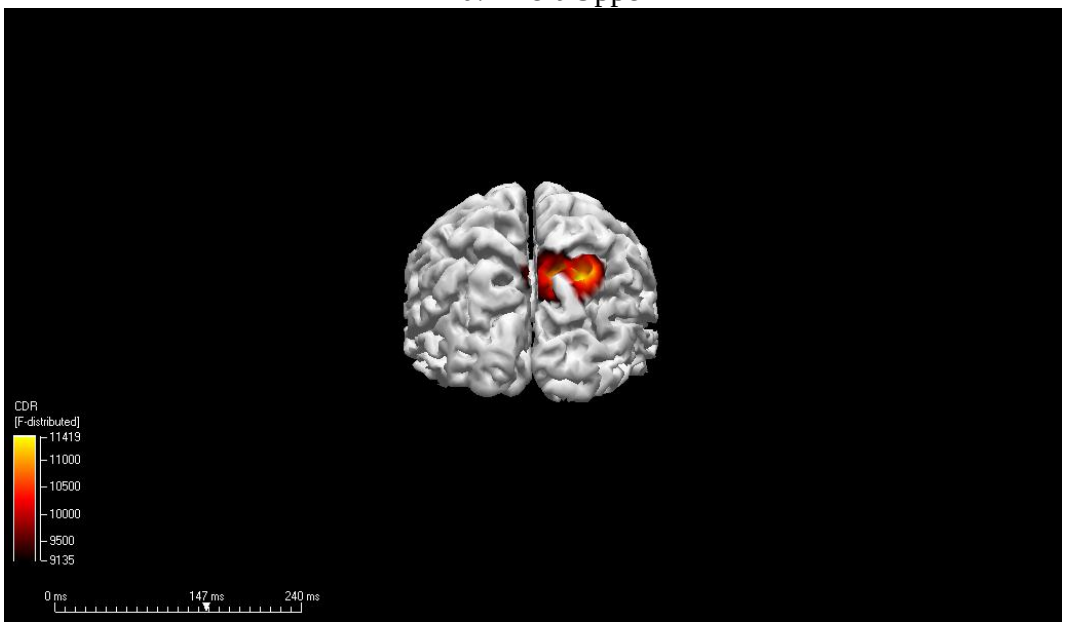

b. Left Lower

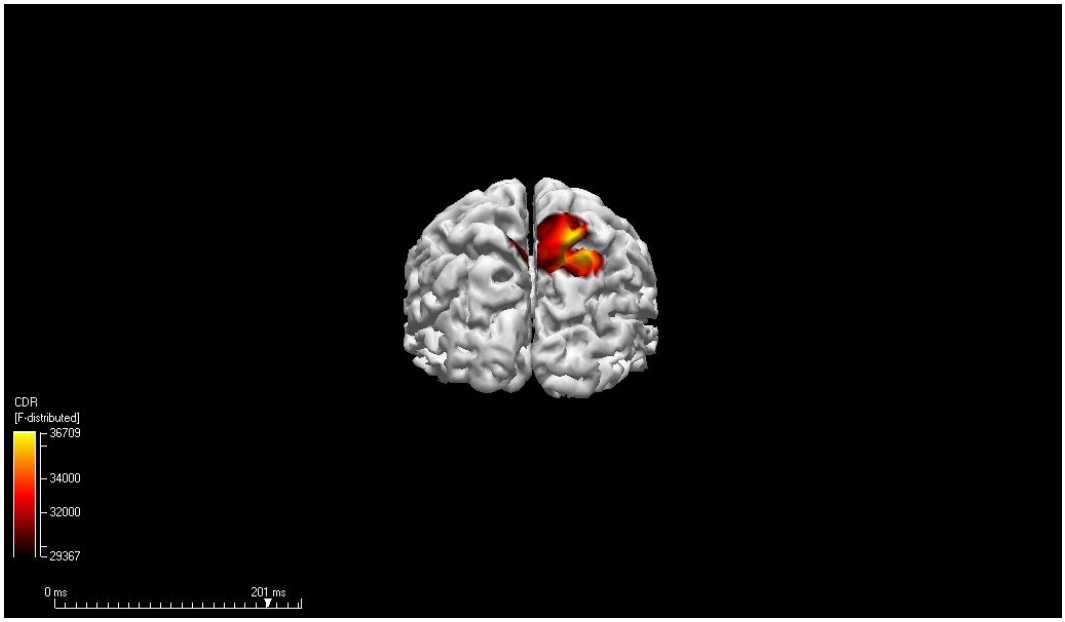

c. Right Upper

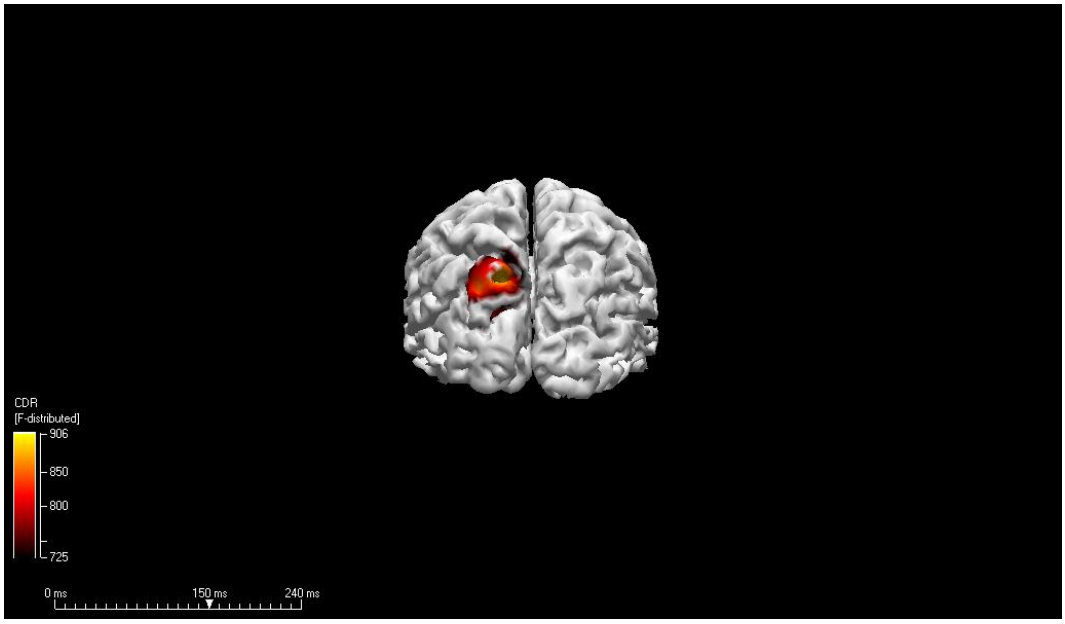

d. Right Lower

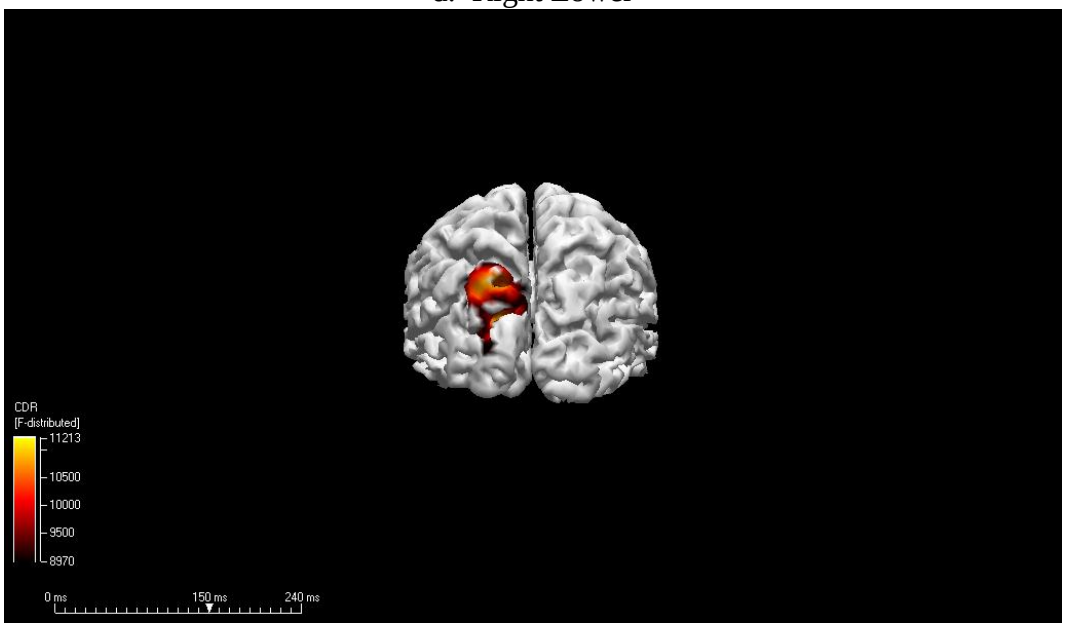

FIGURE 14. sLORETA F values.

a. Left Lower

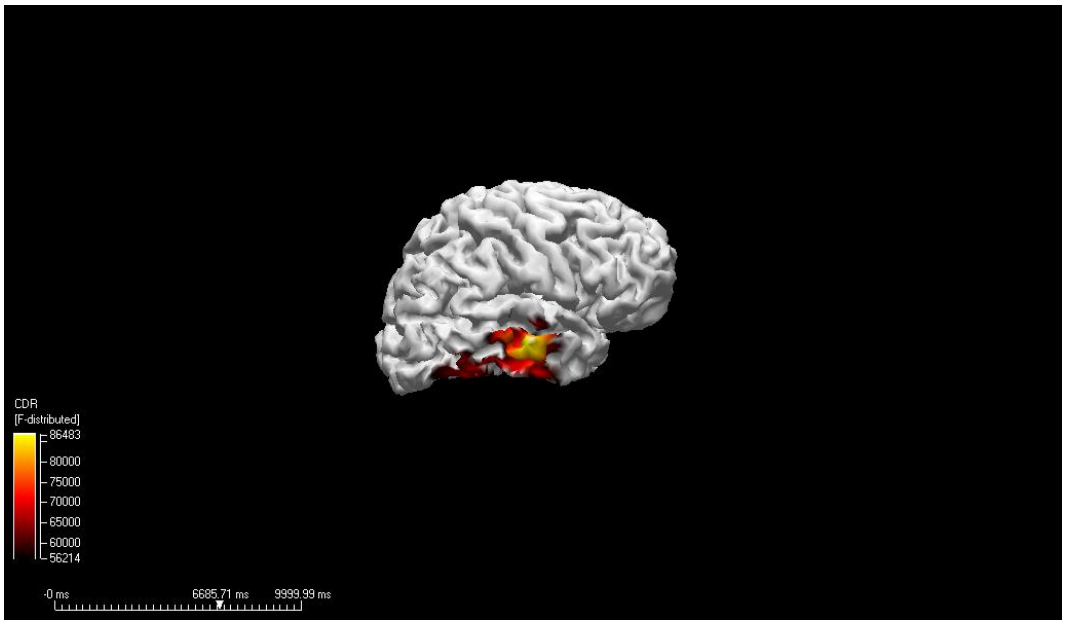

b. Left Lower

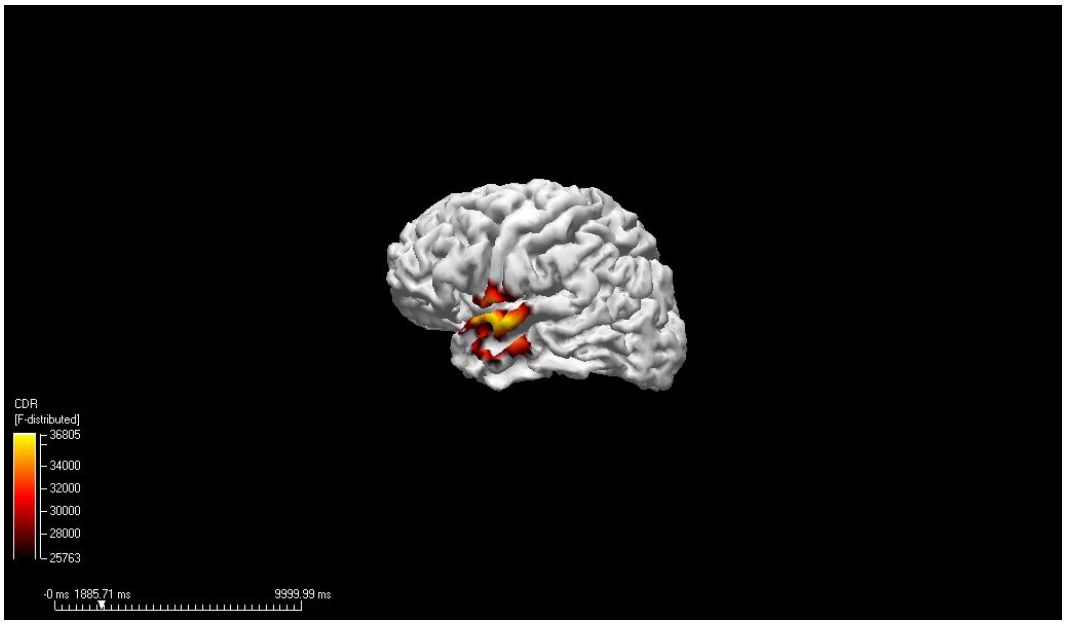

FIGURE 15. sLORETA values.

a. Right Lower .

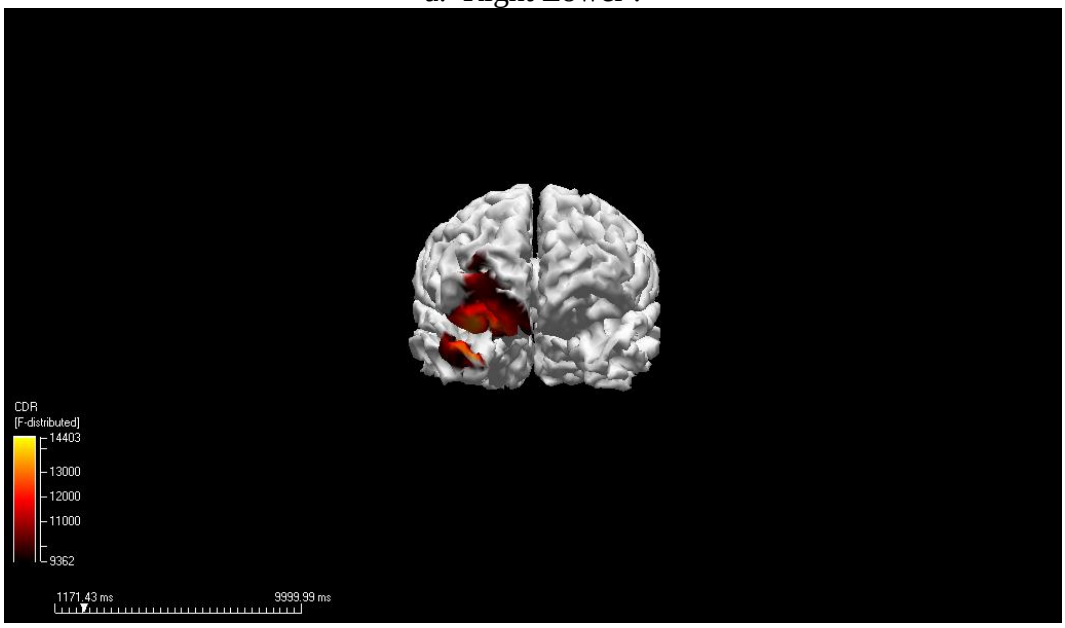

b. Right Lower

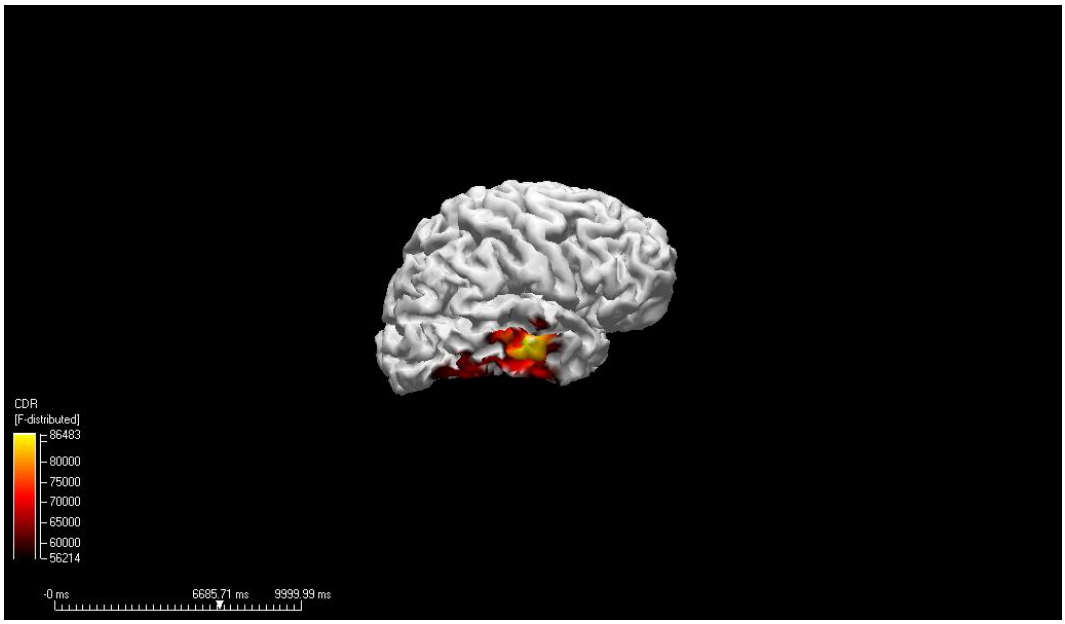

c. Right Upper

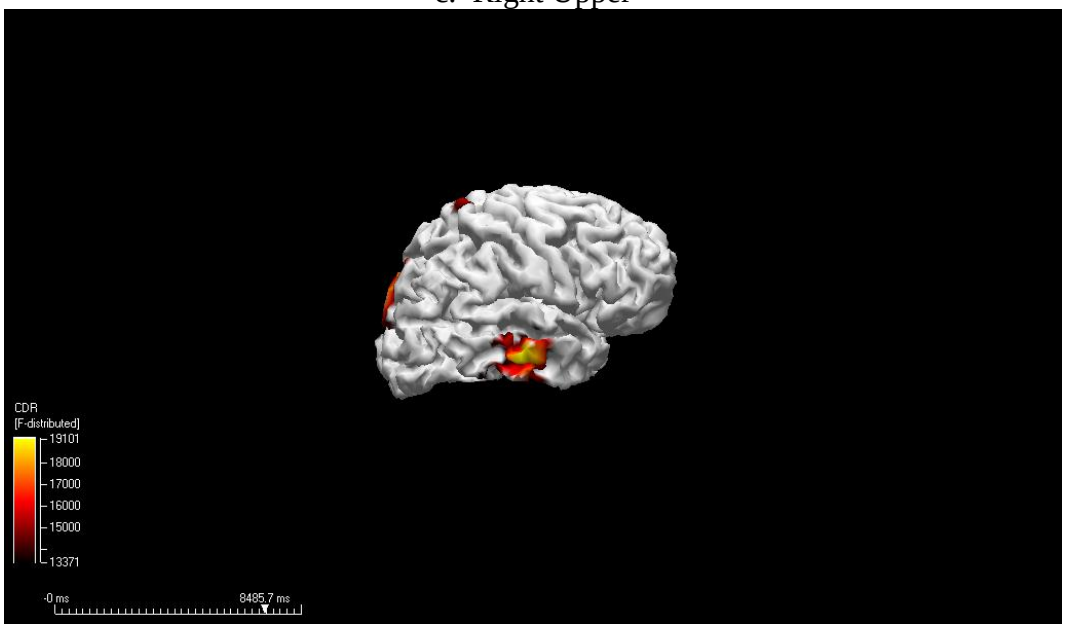

Curriculum Vita

Hugo Sandoval was born and raised in Chihuahua, Mexico, the second son of Hugo Sandoval and Emilia Gonzalez. He received his bachelor's of science in Mechanical Engineering from The University of Texas at El Paso in the summer of 1993. Upon graduating, he returned to work in Chihuahua City where he met Dr. Donald Moss and worked with him in a clinical trial for an Alzheimer's disease medication. This life changing experience encouraged him to pursue his Master's degree in Biological Sciences at The University of Texas at El Paso. He was awarded First Place at the American Society for Microbiology, Rio Grande Branch Graduate Student Research Competition in January 1998. After completing research internships at Sun Health Research Institute in Phoenix and The Mayo Clinic in Jacksonville, Hugo started his Ph.D. studies at the University Of Texas Health Science Center in San Antonio in the Fall of 1999 in the Brain Imaging field. He moved to El Paso in 2005 where he has worked as Director of Business Development for Electrode Arrays and as a Neuromarketing Scientist for Sands Research. Simultaneously, he continued his doctoral studies at the University of Texas at El Paso.

Permanent Address: 1145 Calle Lomas

El Paso, Texas 79912